

بِسْمِ اللَّهِ الرَّحْمَنِ الرَّحِيمِ

DEDICATED TO
DEDICATED TO

*The Holy Prophet (ﷺ) And My Loving Parents
who taught and hold my hands on every step of my
life*

ACKNOWLEDGMENT

In the name of ALLAH the most beneficent and the most merciful. First and foremost, all praises and thanks to Allah Almighty for the strength, courage and His blessing in completing this dissertation. HE who gave me the opportunity, knowledge, ability and help me all the times I needed, without His will I cannot written a single word.

Afterward I offer my humble gratitude to the Holy Prophet MUHAMMAD ﷺ the source of humanity, kindness and guidance for the whole creatures and who declared it an obligatory duty of every Muslim to seek and acquire knowledge.

Then I would like to thanks my family, who are the most important part of my life. I would like to thanks to my parents for their support and love throughout my life. Thank you both for giving me strength to reach for the stars and chase dreams. I have no words to say thanks to my mothers who always support me a lot, built my confidence and pray for me every time. Ammi I am here at this position because of your prayers and support. I am nothing without you. Then I would like to thanks to my sisters (Ifat and Kanwal) and my brother (Faisal) for their support and love.

Being my Supervisor and Chairman of the Department of Mathematics I would like to convey my profound and cordial gratitude to my honourable supervisor Prof. Dr. Tasawar Hayat, who is a source of inspiration for me. I am extremely indebted to my supervisor whose generous suggestions, kind control, guidance, cooperation, encouragement and advices were greatly useful in completing this crucial task. I am also thankful to my respectable teachers of faculty who taught me and guides me.

I gratefully acknowledge the invaluable suggestions and generous guidance of my honorable seniors Dr. M. Farooq, Maimonaapi, Maria api, Anumapi, HinaZahir, Madiha and Sadia Ayub. I also owe my sincere thanks to my research fellows Maryam Shafique, Riya Iqbal, SumairaQayyum, SumairaJabeen, Qurat-ul-Ain and Gulnaz for their suggestions and profilic discussions.

Sadaq Nawaz

Preface

Heat transfer enhancement determines the need for new innovative coolants with improved performance. The new concept of nanofluids has been introduced to make the performance of heat transfer fluids better. The concept of nanofluid has been advanced by S. Choi [1] who showed considerable increase of heat transported in suspensions of copper and aluminium nanoparticles in water and other liquids. Nanofluids are a new kind of fluids which are dispersions of nanoparticles in liquids that are permanently suspended in base fluid. By using different particles which are mostly metals (Cu, Ag, Au), metallic oxides (CuO, Al₂O₃, TiO₂, ZnO), nitride/carbide ceramics (AlN, SiN, SiC, TiC) and carbon nanotubes etc, the engineers created wide range of nanofluids with completely new properties. These heat exchange fluids present interesting heat transfer features when compared with more conventional coolants. Considerable research on thermal conductivity and convective heat transfer of nanofluids is done. In fact, applications of nanofluids such as coolant in automobiles, heat exchangers in industries etc appear promising with these characteristics. Several experimental and theoretical research activities for nanofluids are performed which can be seen through the studies [2-14].

Peristaltic flow refers to the transportation of fluid inside a channel or tube by the action of flexible walls. It is the major mechanism for fluid flow in many biological and industrial systems. Within human body it is involved for swallowing food through esophagus, movement of chyme in the gastro-intestinal track, in the dust efferentes of the male reproductive system, vasomotion of small blood vessels such as arterioles, venules and capillaries etc. Peristaltic pumps are used to transport corrosive or very pure materials so as to avoid direct contact of the fluid with the pump's internal surface. Many biomedical devices such as dialysis machines, open heart bypass pump machines, infusion pumps etc are engineered on the mechanism of peristalsis. Shapiro [15] analyzed the peristaltic pumping in a two dimensional flexible tube. Later on the theoretical results obtained by [15] were confirmed experimentally by Weinberg [16]. Some recent researches dealing with the peristaltic motion are mentioned in the refs. [17-25].

It is well admitted fact that the tubular organs facilitating fluid flow in the human body are internally lubricated with mucus and secretion layer. These layers in turn prevent the fluid from sticking to the walls. In that type of cases the no slip conditions between the fluid and the boundary is not valid. Therefore it seems important to consider slip condition in such

situations. Another important phenomena widely encountered in industrial and engineering applications and attracted the attention of researchers is mixed convection. Ocean current, sea-wind formation, formation of microstructure during the cooling of molten metals etc involve mixed convection. Moreover this phenomenon is utilized in heat exchangers, removal of nuclear waste and in modern cooling /heating system. Having such facts in mind, the present dissertation is arranged as follows.

In the first chapter of this dissertation, explanation of some basic concepts and law relevant to materials utilized in the next two chapters is provided. These basic concepts include peristalsis, nanofluids, heat transfer mechanisms, two phase model for nanofluids, continuity equation, momentum equation, energy equation etc.

The second chapter comprises the work of Shehzadet. al.[38]. In this study the five different nanofluids are considered to discuss the peristaltic transport in a symmetric channel. The two two phase models namely Maxwell and Hamilton-Crosser are considered for the analysis. The study consists of comparison between the results obtained by two phase models. Comparison for the five different water based nanofluids is studied.

In the third chapter, consideration is given to the flow of incompressible water based nanofluid subject to five different types of nanoparticles including metallic and metallic oxides. Here the effects of velocity and thermal slip on the peristaltic transport of nanofluids in asymmetric channel are especially studied. Energy equation is utilized in view of constant heat source /sink parameter. Two thermal conductivity models Maxwell's and Hamilton-Crosser's [44, 45] are used to compare the results for different nanofluids. It is noted that the analysis with above mentioned boundary conditions are not studied yet. Long wavelength and low Reynolds number approximation is utilized. System of coupled equations is solved numerically by using NDSolve in MATHEMATICA. Graphs are sketched to analyze the results.

Peristalsis of Nanoliquids in Presence of Partial Slip Condition



By

Sadaf Nawaz

**Department of Mathematics
Quaid-i-Azam University
Islamabad, Pakistan
2016**

Peristalsis of Nanoliquids in Presence of Partial Slip Condition



By

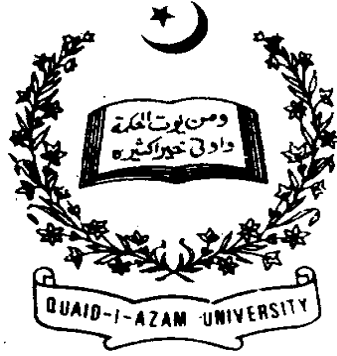
Sadaf Nawaz

Supervised By

Prof. Dr. Tasawar Hayat

**Department of Mathematics
Quaid-i-Azam University
Islamabad, Pakistan
2016**

Peristalsis of Nanoliquids in Presence of Partial Slip Condition



By

Sadaf Nawaz

A thesis submitted in the partial fulfillment of the requirement

for the degree of

MASTER OF PHILOSOPHY

IN

MATHEMATICS

Supervised By

Prof. Dr. Tasawar Hayat

**Department of Mathematics
Quaid-i-Azam University
Islamabad, Pakistan**

2016

Peristalsis of Nanoliquids in Presence of Partial Slip Condition

By

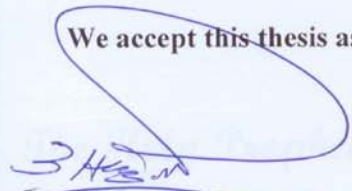
Sadaf Nawaz

CERTIFICATE

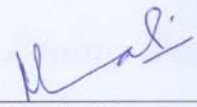
A THESIS SUBMITTED IN THE PARTIAL FULFILLMENT OF THE
REQUIREMENTS FOR THE DEGREE OF THE MASTER OF
PHILOSOPHY

We accept this thesis as conforming to the required standard

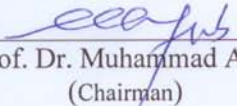
1.


Prof. Dr. Tasawar Hayat
(Supervisor)

2.


Dr. Nasir Ali
(External Examiner)

3.


Prof. Dr. Muhammad Ayub
(Chairman)

**Department of Mathematics
Quaid-i-Azam University
Islamabad, Pakistan
2016**

Contents

1	Fundamental definitions/equations	4
1.1	Basics concepts	4
1.1.1	Fluid	4
1.1.2	Fluid mechanics	4
1.1.3	Fluid density	5
1.1.4	Fluid viscosity	5
1.1.5	Kinematic viscosity	5
1.1.6	Pressure	6
1.1.7	Flow	6
1.1.8	Stream function	7
1.1.9	Real and ideal fluids	7
1.1.10	Newtonian fluids	7
1.1.11	Types of forces	7
1.1.12	Volume flow rate	8
1.1.13	No-slip condition	8
1.1.14	Slip condition	8
1.2	Basics of heat transfer	8
1.2.1	Heat	8
1.2.2	Heat transfer	9
1.2.3	Mechanisms of heat transfer	9
1.2.4	Specific heat	10
1.2.5	Thermal conductivity	10

1.2.6	Viscous dissipation	10
1.3	Peristalsis	11
1.3.1	Peristalsis in physiology	11
1.3.2	Pumping	11
1.4	Nanofluids and Nanoparticles	12
1.4.1	Nanoparticles	12
1.4.2	Nanofluids	12
1.4.3	Two phase thermal conductivity models of nanofluids	13
1.5	Dimensionless numbers	14
1.5.1	Reynolds number	14
1.5.2	Wave number	14
1.5.3	Prandtl number	14
1.5.4	Eckert number	15
1.5.5	Brinkman number	15
1.5.6	Grashof number	15
1.6	Basic Equations for flow analysis	15
1.6.1	Continuity equation	16
1.6.2	Momentum equation	16
1.6.3	Energy equation	16
2	Peristaltic motion of water-based nanomaterials	18
2.1	Introduction	18
2.2	Physical model	18
2.3	Problem formulation	20
2.3.1	Non-dimensionalization	24
2.4	Discussion	26
2.4.1	Analysis of velocity profile	28
2.4.2	Analysis of temperature profile	28
2.4.3	Heat transfer rate	28

3	A model for an application to biomedical engineering through nanoparticles	35
3.1	Introduction	35
3.2	Mathematical formulation	36
3.3	Analysis and discussion	41
3.4	Conclusions	58

Chapter 1

Fundamental definitions/equations

The basic aim of this chapter is to provide some basic concepts and equations that will be helpful for the better understanding of analysis in the subsequent chapters.

1.1 Basics concepts

1.1.1 Fluid

Fluid is defined as a substance that has not a definite shape and deforms continuously under the action of shear stress no matter how small is it. Mainly fluids show the two characteristics i.e. not resisting deformation, or slightly resisting because of (viscosity) and the fluidity (ability to flow) property.

1.1.2 Fluid mechanics

The branch in which consideration is given to the mechanics of fluid and the applied forces on them. It is further subdivided into two parts defined as follows:

Fluid dynamics

The branch that deals with the studies when the fluid is in motion is named as fluid dynamics.

Fluid statics

The branch that deals with the situation when the fluid is not in motion is named as fluid statics.

1.1.3 Fluid density

The density of the fluid represented by the greek symbol ρ is defined as the mass per unit volume at specific temperature and pressure. Mathematical expression to define the density at the point are given by:

$$\rho = \lim_{\delta \rightarrow 0} \left(\frac{\delta m}{\delta v} \right). \quad (1.1)$$

Here δm is use to describe the mass element whereas δv represents the volume element.

1.1.4 Fluid viscosity

Viscosity of the fluid in common language known as thickness of the fluid. It is the inherent property of fluid that measures the resistance offered by the fluid during flow under the action of shear stress. In nature all the fluids found has the viscosity effects. Mathematically, the expression for viscosity is denoted by the symbol μ which is known as dynamic viscosity or absolute viscosity and is defined by

$$\text{Viscosity } (\mu) = \frac{\text{shear stress}}{\text{shear rate/deformation rate}}, \quad (1.2)$$

The unit and dimension of viscosity in SI system is given by Pascal. sec ($Pa.s$) or $kg/m.s$ and $[M/LT]$ respectively.

1.1.5 Kinematic viscosity

Ratio of absolute viscosity (μ) to the density of the fluid is named as kinematic viscosity represented by the symbol ν . Mathematically given by

$$\nu = \frac{\mu}{\rho}. \quad (1.3)$$

The unit and dimension of kinematic viscosity in SI system is given by m^2/s and dimension $[L^2/T]$.

1.1.6 Pressure

Pressure is defined as the magnitude of the force per unit area. Mathematical relation for pressure is given by:

$$Pressure = \frac{\text{Magnitude of applied force}}{\text{area}} = \frac{|F|}{A}. \quad (1.4)$$

1.1.7 Flow

A material that show deformation when it is under the influence of various type of forces. If the material started continuously deforming without any restriction then that type of phenomena is know as flow.

Steady flow

Steady flow are described as the flow in which properties of the fluid are not a function of time.

Unsteady flow

Unsteady flow are described as the flow in which properties of the fluid are a function of time.

Compressible flow

A compressible flow is defined as flow whose density changes with respect to the space and time coordinates.

Incompressible flow

An incompressible flow is defined as flow whose density remain unchanged with respect to the space and time coordinates.

1.1.8 Stream function

Stream function is defined as a function which describes the form of flow pattern or we can state that it is the discharge per unit thickness. It is use to illustrate the flow field in terms of volume flow rate for incompressible fluid and mass flow rate for compressible flow. For the case of two dimensional steady flow relation is given by

$$V = \nabla \times \psi, \quad (1.5)$$

The velocity components can be described in terms of constant stream function as

$$u = \frac{\partial \psi}{\partial y}, \quad v = -\frac{\partial \psi}{\partial x}. \quad (1.6)$$

1.1.9 Real and ideal fluids

Real and ideal fluids are distinguish on the basic of viscosity of the fluid. Ideal fluids are characterized by the zero viscosity effects. These type of fluids does not show any resistance against flow. On the other hand the fluids which exhibit the viscosity effects are named as real fluid. In nature no ideal fluid exist and all the fluid are real. Examples including water, milk, blood, air, paints, toothpaste etc. Real fluids are subdivide into two types namely Newtonian or viscous fluid and non-Newtonian fluids.

1.1.10 Newtonian fluids

The fluid are named as Newtonian fluids, which obeys the "Newton's law of viscosity" which states that the shear stress is in direct and linearly proportion to deformation rate.

1.1.11 Types of forces

Surface forces

Forces that applied on external surface or internal element of the material. These type of forces has direct contact with the surface. Surface forces has further two types, pressure forces that is applied normal to the surface and stress forces that is applied in tangential direction.

Body forces

Body forces are described as the forces that does not have direct contact with the material and acts on the control volume. Magnetic force and gravity are example of body forces.

1.1.12 Volume flow rate

When the fluid of volume Q moves from the section of pipe. The fluid is moving with velocity V and constructing an angle θ with the normal to A , then in this case volume flow rate is defined as:

$$Q = AV \cos \theta. \quad (1.7)$$

In the case when flow is normal to A then we have $\theta = 0$, and the volume flow rate become:

$$Q = AV. \quad (1.8)$$

1.1.13 No-slip condition

When the fluid adjacent to the boundary stick with the boundary i.e. the relative velocity between the fluid and boundary is zero. This situation is termed as no-slip condition. In that type of situations adhesive forces are dominant than the cohesive forces.

1.1.14 Slip condition

Sometimes in the case of permeable wall, coated surfaces etc. the relative velocity of the fluid and the boundary is not zero. Which means that the fluid attached with the boundary moves with different velocity as that of the wall. This situation is termed as slip condition. In that type of situations cohesive forces are dominant than the adhesive forces.

1.2 Basics of heat transfer

1.2.1 Heat

Heat is a form of energy that travel from high temperature region to the region with low temperature.

1.2.2 Heat transfer

Heat transfer phenomena consist of transfer of energy between the body located at different temperature. This is an important phenomena and are utilized in many processes. For example this principle is utilized in heat exchangers, refrigerating and in chemical processes. Principle of heat transfer can be applied to human body. Because our body has to maintain a healthy temperature that is $37^{\circ}F$ to keep working the organs properly and to avoid the body from overheating. So extra heat must be dissipated through the body which is produced through metabolisms.

1.2.3 Mechanisms of heat transfer

When the two bodies are located with different temperature then the heat always move from the body with higher temperature to one with lower temperature. The transfer of heat is done by the three mechanisms (modes) as defined below:

Conduction

In this mode, heat transfer between two bodies in direct contact is done through the collusion of molecules. In this process the molecules with high energy transmit energy to molecules with low energy. So this process carry on without the transfer of molecules from one place to another.

Convection

In this type of mechanisms heat is transfer via transfer of mass. In this process heat is transfer via molecules transfer. Convection has further three types as given below:

Natural convection Natural convection which is also referred to as free convection. In this type of mechanism, heat is transfer due to the variation in temperature which also effect the density of the fluid when the gravity is present.

Force convection In this type of mechanism some external agent for example fan, pump or stirrers is responsible for the motion of fluid that help in transfer heat. This type of process is necessary for enhancing the heat transfer rate.

Mixed convection When the transfer of heat is done through the combined effects of natural and forced convection then it is named as mixed convection. This type of mechanism of heat transfer is seen to be useful and are utilized in many engineering devices and process like heat exchangers, nuclear reactor etc.

Radiation

This type of mechanism comprises of transfer of heat via emission and absorption of electromagnetic waves. Sun is one of the common example where heat is transfer through the radiation. In our home use of micro-oven also lie in this category in which the radiations are used to heat the food. Convection and radiation are the prominent mechanisms of heat transfer in the liquids and gases whereas in solids conduction is the prominent mechanism.

1.2.4 Specific heat

It is defined as the amount of energy needed to raise the temperature of the body to one degree Celsius.

1.2.5 Thermal conductivity

It is related to the property of the material to conduct heat. Higher the value of thermal conductivity means that more heat will flow through the material whereas less heat will flow through the material when the thermal conductivity of the material is low. Due to these advantages materials with high thermal conductivity are utilized in heat sink applications whereas in thermal insulations materials with low thermal conductivity are utilized. In SI system the unit of thermal conductivity is given by $W/m.K$ or kgm/s^3K whose dimension is given by $[ML/T^3\theta]$.

1.2.6 Viscous dissipation

The phenomena in the flow configuration due to the viscous force is known as viscous dissipation. In this phenomena due to viscous forces mechanical energy is dissipated into internal energy of the material.

1.3 Peristalsis

The word peristalsis has its roots from the Greek word "Peristaltikos" which means "clasping and compressing". It is the mechanism in which due to the contraction and expansion of waves fluid moves.

"A successive waves of involuntary contraction and expansion passing along the walls of a hollow muscular structure and forcing the contents onward"

1.3.1 Peristalsis in physiology

Phenomena of peristalsis is extensively found in the human body where the basic purpose is the transportation of fluid from one part to the other part of body. It is involve in the transport of food through the oesophagus, in lymph transport, urine transport from kidney to gall bladder etc.

1.3.2 Pumping

The phenomena of peristalsis comprises of transportation of material from lower pressure gradient to one with high pressure gradient. This phenomena is named as pumping.

Positive and negative pumping

On the basis of dimensionless mean flow rate η the positive and negative pumping is characterized. The pumping is positive when the flow rate is positive and negative when the flow rate is negative.

Adverse and favorable pressure gradient

Adverse pressure occurs when pressure is in the direction of flow i.e. pressure rise per wavelength (ΔP_λ) is positive otherwise it is named as favourable pressure gradient.

Peristaltic pumping

Peristaltic pumping depends positive flow rate ($\eta > 0$) and adverse pressure gradient ($\Delta P_\lambda > 0$).

Augmented pumping

Augmented pumping is characterized by the positive flow rate ($\eta > 0$) and favourable pressure gradient ($\Delta P_\lambda < 0$).

Retrograde pumping

Retrograde pumping depends on the negative flow rate ($\eta < 0$) and adverse pressure gradient ($\Delta P_\lambda > 0$).

Free pumping

Free pumping is characterized by the positive flow rate ($\eta > 0$) and pressure rise is neither favourable nor adverse ($\Delta P_\lambda = 0$).

1.4 Nanoliquids and Nanoparticles

1.4.1 Nanoparticles

Nanoparticles are characterized as the particles having the size between 1-100 nm. These particles have different shapes like spherical, cylindrical, tube like etc. and made up of different materials like metals (*Cu, Fe, Ag, Au*), metallic oxides (*CuO, Al₂O₃, TiO₂, Fe₃O₄*), Carbides/nitrides (*AlN, SiN, SiC, TiC*), single and multiwalled nanotubes etc. Use of metallic particles and SWCNT and MWCNT are very common in cooling process as they have high thermal conductivity value.

1.4.2 Nanoliquids

The suspension comprising of nanoparticles plus base fluid is named as nanoliquid or nanofluid. These types of fluid have distinct mechanical properties when compared to fluid prepared by utilizing the large size particles (micro or macro size) of the same material. One of the prominent feature of this type of fluid is the enhance capability of heat transfer as compared to other traditional fluids. The base fluid used in the nanofluid are commonly water, ethylene-glycol, oil etc. and the nanoparticles used are commonly metallic, metallic oxides and nanotubes etc. Due

to enhance capability of heat transfer nanofluid are utilized in many engineering and industrial applications. For example nanofluid are widely used as the coolant in automobiles to reduced the internal combustion of engine. One of the other use of nanofluids is in the cooling of nuclear reactors, electronic cooling etc.

1.4.3 Two phase thermal conductivity models of nanofluids

Many models of thermal conductivity were given by researchers to estimate the thermal conductivity of the nanofluid consisting of continuous and discontinuous phase. Some of the two phase models utilized in this dissertation are given below:

Maxwell model

Thermal conductivity model given by Maxwell is comprised of the thermal conductivity of the nanoparticle having spherical shape and the base fluid thermal conductivity. The effective thermal conductivity for this model is given by

$$\frac{K_{eff}}{K_f} = \frac{K_p + 2K_f - 2\phi(K_f - K_p)}{K_p + 2K_f + \phi(K_f - K_p)}, \quad (1.9)$$

here K_p and K_f elucidate the thermal conductivity of the respective nanoparticles and base fluid.

Hamilton-Crosser's model

Extension on Maxwell model was done by Hamilton and Crosser and model was given to cover the non-spherical particles. A factor n is included in the model which is given by $n = 3/\Psi$, where Ψ illustrates the sphericity of the particles included in the nanofluid. $\Psi = 1$ corresponds to the spherical particles and in this case two models coincide. The effective thermal conductivity for this model is given by

$$\frac{K_{eff}}{K_f} = \frac{K_p + (n-1)K_f - (n-1)\phi(K_f - K_p)}{K_p + (n-1)K_f + \phi(K_f - K_p)}, \quad (1.10)$$

here K_p and K_f elucidate the thermal conductivity of the respective nanoparticles and base fluid.

1.5 Dimensionless numbers

1.5.1 Reynolds number

Reynolds number denoted by Re is defined as the ratio of inertial to viscous forces. It is used to give information whether the fluid flow is laminar or turbulent. At low value of Reynolds number where the viscous forces are dominant the fluid is characterized as laminar. For laminar flow the Reynolds number range is < 2000 . For turbulent flow the inertial forces are dominant so the value of Reynolds number is high. Here in this case the Reynolds number range is > 4000 . The range between these values is named as transition phase. Mathematical expression for Reynolds number is given by

$$Re = \frac{\textit{inertial forces}}{\textit{viscous forces}} = \frac{\rho cd}{\mu}, \quad (1.11)$$

here ρ depicts the density of the fluid where c and d are characterized as the velocity and length scale respectively.

1.5.2 Wave number

The ratio of width of channel to its wavelength is named as wave number. Mathematical expression for the wave number is as follows:

$$\delta = \frac{d}{\lambda}. \quad (1.12)$$

1.5.3 Prandtl number

A dimensionless quantity appeared in the analysis which was named on the German pioneer physicist Ludwig Prandtl. Prandtl number is defined as the ratio of momentum diffusivity and thermal diffusivity. Mathematically denoted as

$$Pr = \frac{\textit{momentum diffusivity}}{\textit{thermal diffusivity}} = \frac{\mu C_p}{K}, \quad (1.13)$$

in the above equation the quantity μ is the viscosity, C_p is specific heat whereas K describes the fluid thermal conductivity.

1.5.4 Eckert number

This dimensionless number appears due to the viscous dissipation effects in the fluid. It is represented as the ratio of kinetic energy to the enthalpy. It was named after Ernst R. G. Eckert. Mathematically given by

$$Ec = \frac{\textit{kinetic energy}}{\textit{enthalpy}} = \frac{c^2}{C_p(T_1 - T_0)}. \quad (1.14)$$

The viscous dissipation effects are negligible effects for low values of Eckert number ($Ec \ll 1$).

1.5.5 Brinkman number

It illustrates the ratio of viscous dissipation to the heat transfer through conduction. It is given by the product of Prandtl and Eckert number.

$$Br = Pr Ec \quad (1.15)$$

1.5.6 Grashof number

Grashof number is defined as the ratio of buoyancy to viscous forces. It was pronounced as Grashof number after the German engineer Franz Grashof. Mathematical expression is given by

$$Gr = \frac{\textit{buoyant forces}}{\textit{viscous forces}} = \frac{g\beta_T(T_1 - T_0)d^2}{\nu c}, \quad (1.16)$$

here g and β_T represent the acceleration due to gravity and thermal expansion coefficient respectively.

1.6 Basic Equations for flow analysis

The following basic equation are utilized in this dissertation.

- Equation of continuity
- Momentum equation
- Energy equation

1.6.1 Continuity equation

Continuity equation is derived from the law of conservation of mass which states that the rate through which mass is entering in the system is equal to the rate through which mass is leaving. Mathematically, defined as

$$\frac{\partial \rho}{\partial t} + \text{div}(\rho \mathbf{V}) = 0, \quad (1.17)$$

where in the expression used in above equation defines ρ the density, \mathbf{V} the velocity vector for the fluid given by $\mathbf{V} = [U, V, W]$. For the case of incompressible fluid $\rho = \text{constant}$, continuity equation takes the form as:

$$\text{div } \mathbf{V} = 0, \quad (1.18)$$

or

$$\nabla \cdot \mathbf{V} = 0. \quad (1.19)$$

The above mentioned equation is only applicable to the case when source/sink is absent and volume is controlled one.

1.6.2 Momentum equation

This equation comes from the law of conservation of the linear momentum. Mathematically given in vector form:

$$\rho \frac{d\mathbf{V}}{dt} = \text{div } \mathbf{S} + \rho \mathbf{b}, \quad (1.20)$$

here \mathbf{S} denotes the Cauchy stress tensor and \mathbf{b} is used to represent the body force. The material derivative represented by $\frac{d}{dt}$ is defined as

$$\frac{d}{dt} = \frac{\partial}{\partial t} + \mathbf{V} \cdot \nabla. \quad (1.21)$$

1.6.3 Energy equation

The energy equation is derived from first law of thermodynamics which states that

"The change in total energy of the system is equal to the amount of heat added to the system minus workdone by the system on the surrounding."

The energy equation for the flow configuration is given by:

$$\rho C_p \left(\frac{\partial}{\partial t} + \mathbf{v} \cdot \nabla \right) T = K \nabla^2 T + \mathbf{S} \cdot \mathbf{L}. \quad (1.22)$$

Here ρ denotes the density, C_p the specific heat whereas K is used for the thermal conductivity of the fluid. Also the term $\mathbf{S} \cdot \mathbf{L}$ represents the viscous dissipation effect.

Chapter 2

Peristaltic motion of water-based nanomaterials

2.1 Introduction

In this chapter consideration is given to the peristaltic transport of nanofluid in a vertical symmetric channel. Water based nanofluids are utilized here. Base fluid here is considered water. The considered nanoparticles are Titanium oxide or titania (TiO_2), Aluminum oxide or Alumina (Al_2O_3), Copper oxide (CuO), Copper (Cu) and Silver (Ag). Two effective thermal conductivity models namely Maxwell and Hamilton-Crosser's are employed. Energy equation includes viscous dissipation and heat generation/absorption. Moreover study has been carried out not only by applying long wavelength but also by considering low Reynolds number assumption. Solution of the considered problem is developed by using NDSolve of MATHEMATICA. Graphical results are analyzed for different embedded parameters involved in the problem. This chapter comprises of detailed review of a paper by Shehzad et al. [38].

2.2 Physical model

We examine the two dimensional flow of an incompressible nanofluid in a symmetric vertical channel of width $2d$. Flow is induce in the channel because of the sinusoidal waves having the small amplitude a_1 and long wavelength λ . Selection of rectangular coordinates system

(\bar{X}, \bar{Y}) is done in such a manner that \bar{X} -axis lies along the length of channel where wave is propagating and \bar{Y} -axis lies in the direction normal to \bar{X} -axis (see Fig. 2.1).

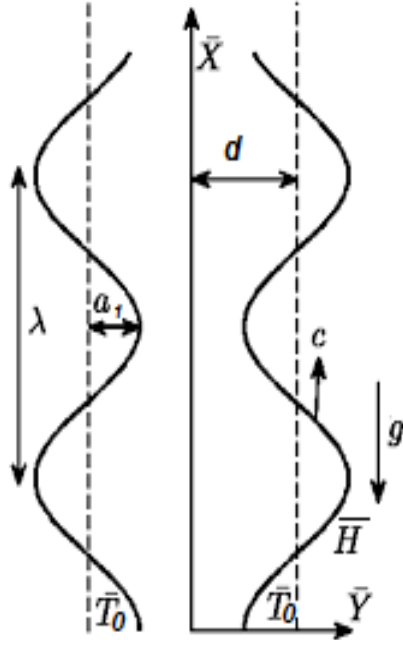


Fig 2.1: Schematic Diagram

The walls of the channel are described by the expression

$$\bar{Y} = \bar{H}(\bar{X}, \bar{t}) = d + a_1 \cos \frac{2\pi}{\lambda} (\bar{X} - c\bar{t}) \quad \text{at right wall,} \quad (2.1)$$

$$\bar{Y} = -\bar{H}(\bar{X}, \bar{t}) = -\left[d + a_1 \cos \frac{2\pi}{\lambda} (\bar{X} - c\bar{t}) \right] \quad \text{at left wall.} \quad (2.2)$$

Here \bar{H} is the wall displacement, d is the half width of the considered symmetric channel, a_1 describes the amplitude with which the wave is travelling whereas speed and wavelength of the wave are represented by c and λ respectively. For the considered flow configuration the two dimensional velocity field \mathbf{V} is given by

$$\mathbf{V} = [\bar{U}(\bar{X}, \bar{Y}, \bar{t}), \bar{V}(\bar{X}, \bar{Y}, \bar{t}), 0], \quad (2.3)$$

where $\bar{U}(\bar{X}, \bar{Y}, \bar{t})$ and $\bar{V}(\bar{X}, \bar{Y}, \bar{t})$ are the respective velocity components in the longitudinal and transverse directions in the fixed frame of reference.

2.3 Problem formulation

The basic equations for the incompressible nanofluid are

$$\operatorname{div} \mathbf{V} = 0, \quad (2.4)$$

$$\rho_{eff} \frac{d\mathbf{V}}{dt} = \operatorname{div} \mathbf{S} + g(\rho\beta)_{eff} (T - T_0), \quad (2.5)$$

$$(\rho C)_{eff} \frac{dT}{dt} = K_{eff} \nabla^2 T + \mathbf{S} \cdot \mathbf{L} + \Phi. \quad (2.6)$$

In the above mentioned equations \mathbf{V} represents the velocity, ρ_{eff} denotes effective density of the nanofluid, \mathbf{S} is used for the Cauchy stress tensor, g the gravitational acceleration, $(\rho\beta)_{eff}$ denotes the effective thermal expansion coefficient for nanofluid, $(\rho C)_{eff}$ the effective heat capacity, K_{eff} the effective thermal conductivity of the nanofluid and the material time derivative $\frac{d}{dt}$ is given by

$$\frac{d}{dt} = \frac{\partial}{\partial t} + \bar{U} \frac{\partial}{\partial \bar{X}} + \bar{V} \frac{\partial}{\partial \bar{Y}}. \quad (2.7)$$

The Cauchy stress tensor \mathbf{S} for the case of viscous incompressible nanofluid is

$$\mathbf{S} = -\bar{P} \mathbf{I} + \mu_{eff} \mathbf{A}_1, \quad (2.8)$$

here \bar{P} depicts the pressure, \mathbf{I} symbolizes the identity tensor, μ_{eff} the effective viscosity whereas \mathbf{A}_1 shows the first Rivlin-Ericksen tensor defined as

$$\mathbf{A}_1 = \mathbf{L} + \mathbf{L}^T, \quad (2.9)$$

where

$$\mathbf{L} = (\operatorname{grad} \mathbf{V}), \quad (2.10)$$

where superscript T depict the transpose of \mathbf{L} . Now we have

$$\mathbf{L} = \begin{bmatrix} \bar{U}_x & \bar{U}_y & 0 \\ \bar{V}_x & \bar{V}_y & 0 \\ 0 & 0 & 0 \end{bmatrix}, \quad \mathbf{L}^T = \begin{bmatrix} \bar{U}_x & \bar{V}_x & 0 \\ \bar{U}_y & \bar{V}_y & 0 \\ 0 & 0 & 0 \end{bmatrix}, \quad (2.11)$$

In view of Eq. (2.9), we get

$$\mathbf{A}_1 = \begin{bmatrix} 2\bar{U}_x & \bar{U}_y + \bar{V}_x & 0 \\ \bar{V}_x + \bar{U}_y & 2\bar{V}_y & 0 \\ 0 & 0 & 0 \end{bmatrix}. \quad (2.12)$$

Now substituting the obtained value of \mathbf{A}_1 mentioned above in Eq. (2.8) we obtained

$$\mathbf{S} = \begin{bmatrix} -\bar{P} + 2\mu_{eff}\bar{U}_x & \mu_{eff}(\bar{U}_y + \bar{V}_x) & 0 \\ \mu_{eff}(\bar{U}_y + \bar{V}_x) & -\bar{P} + 2\mu_{eff}\bar{V}_y & 0 \\ 0 & 0 & 0 \end{bmatrix}. \quad (2.13)$$

Moreover

$$\mathbf{S} \cdot \mathbf{L} = tr(\mathbf{S}\mathbf{L}) = \bar{U}_x S_{xx} + S_{xy}(\bar{U}_y + \bar{V}_x) + \bar{V}_y S_{yy}. \quad (2.14)$$

After putting all the values calculated in Eqs. (2.8) – (2.14), the continuity, momentum, and energy equations in the presence of body force take the form as define below

$$\frac{\partial \bar{U}}{\partial \bar{X}} + \frac{\partial \bar{V}}{\partial \bar{Y}} = 0, \quad (2.15)$$

$$\rho_{eff} \left(\frac{\partial}{\partial \bar{t}} + \bar{U} \frac{\partial}{\partial \bar{X}} + \bar{V} \frac{\partial}{\partial \bar{Y}} \right) \bar{U} = -\frac{\partial \bar{P}}{\partial \bar{X}} + \mu_{eff} \left[\frac{\partial^2 \bar{U}}{\partial \bar{X}^2} + \frac{\partial^2 \bar{U}}{\partial \bar{Y}^2} \right] + g(\rho\beta)_{eff} (T - T_0), \quad (2.16)$$

$$\rho_{eff} \left(\frac{\partial}{\partial \bar{t}} + \bar{U} \frac{\partial}{\partial \bar{X}} + \bar{V} \frac{\partial}{\partial \bar{Y}} \right) \bar{V} = -\frac{\partial \bar{P}}{\partial \bar{Y}} + \mu_{eff} \left[\frac{\partial^2 \bar{V}}{\partial \bar{X}^2} + \frac{\partial^2 \bar{V}}{\partial \bar{Y}^2} \right], \quad (2.17)$$

$$\begin{aligned} (\rho C)_{eff} \left(\frac{\partial}{\partial \bar{t}} + \bar{U} \frac{\partial}{\partial \bar{X}} + \bar{V} \frac{\partial}{\partial \bar{Y}} \right) T &= K_{eff} \left[\frac{\partial^2 T}{\partial \bar{X}^2} + \frac{\partial^2 T}{\partial \bar{Y}^2} \right] + \Phi \\ &+ \mu_{eff} \left[\begin{array}{l} 2 \left(\left(\frac{\partial \bar{U}}{\partial \bar{X}} \right)^2 + \left(\frac{\partial \bar{V}}{\partial \bar{Y}} \right)^2 \right) \\ + \left(\frac{\partial \bar{U}}{\partial \bar{Y}} + \frac{\partial \bar{V}}{\partial \bar{X}} \right)^2 \end{array} \right], \end{aligned} \quad (2.18)$$

The quantities ρ_{eff} , $(\rho C)_{eff}$, $(\rho\beta)_{eff}$ and μ_{eff} for the two phase flow model are defined as

$$\begin{aligned}\rho_{eff} &= (1 - \phi)\rho_f + \phi\rho_p, & (\rho C)_{eff} &= (1 - \phi)(\rho C)_f + \phi(\rho C)_p, \\ (\rho\beta)_{eff} &= (1 - \phi)\rho_f\beta_f + \phi\rho_p\beta_p, & \mu_{eff} &= \frac{\mu_f}{(1 - \phi)^{2.5}}.\end{aligned}\quad (2.19)$$

The expression for the effective thermal conductivity of nanofluid for Maxwell [44] and Hamilton-Crosser's [45] models are

$$\frac{K_{eff}}{K_f} = \frac{K_p + 2K_f - 2\phi(K_f - K_p)}{K_p + 2K_f + \phi(K_f - K_p)}, \quad (2.20)$$

$$\frac{K_{eff}}{K_f} = \frac{K_p + (n - 1)K_f - (n - 1)\phi(K_f - K_p)}{K_p + (n - 1)K_f + \phi(K_f - K_p)}, \quad (2.21)$$

where K_p and K_f describe the thermal conductivities for nanoparticles and base fluid. Moreover $n = 3/\Psi$ where Ψ define the sphericity of the nanoparticles used in the nanofluid. Hamilton-Crosser model for $n = 3$ becomes Maxwell model.

The boundary conditions for the flow configuration are given by

$$\frac{\partial \bar{U}}{\partial \bar{Y}} = 0 \quad \text{at } \bar{Y} = 0, \quad (2.22)$$

$$\bar{U} = 0 \quad \text{at } \bar{Y} = \bar{H}(\bar{X}, \bar{t}) = d + a_1 \cos \frac{2\pi}{\lambda} (\bar{X} - c\bar{t}), \quad (2.23)$$

$$\frac{\partial T}{\partial \bar{Y}} = 0 \quad \text{at } \bar{Y} = 0, \quad (2.24)$$

$$T = T_0 \quad \text{at } \bar{Y} = \bar{H}(\bar{X}, \bar{t}) = d + a_1 \cos \frac{2\pi}{\lambda} (\bar{X} - c\bar{t}). \quad (2.25)$$

Numerical values of the thermo-physical parameters of water and nanoparticles are mentioned in Table 1.

Table 1: Thermo-physical parameters of water and nanoparticles

	ρ (kg m ⁻³)	C_p (j kg ⁻¹ K ⁻¹)	K (W m ⁻¹ K ⁻¹)	β (1/k) $\times 10^{-6}$
H ₂ O	997.1	4179	0.613	210
TiO ₂	4250	686.2	8.9538	9.0
Al ₂ O ₃	3970	765	40	8.5
CuO	6320	531.8	76.5	18.0
Cu	8933	385	401	16.7
Ag	10500	235	429	18.9

To transform our system from laboratory to wave frame of reference the transformation between two frames are given by

$$\begin{aligned}\bar{x} &= \bar{X} - c\bar{t}, \quad \bar{y} = \bar{Y}, \quad \bar{u}(\bar{x}, \bar{y}) = \bar{U}(\bar{X}, \bar{Y}, \bar{t}) - c, \\ \bar{v}(\bar{x}, \bar{y}) &= \bar{V}(\bar{X}, \bar{Y}, \bar{t}), \quad \bar{p}(\bar{x}, \bar{y}) = \bar{P}(\bar{X}, \bar{Y}, \bar{t}),\end{aligned}\tag{2.26}$$

here $\bar{u}(\bar{x}, \bar{y})$, $\bar{v}(\bar{x}, \bar{y})$ and $\bar{p}(\bar{x}, \bar{y})$ are the velocity components and pressure in the wave frame respectively. After utilizing these transformation our system of equations take the form

$$\frac{\partial \bar{u}}{\partial \bar{x}} + \frac{\partial \bar{v}}{\partial \bar{y}} = 0,\tag{2.27}$$

$$\begin{aligned}((1 - \phi)\rho_f + \phi\rho_p) \left((\bar{u} + c)\frac{\partial}{\partial \bar{x}} + \bar{v}\frac{\partial}{\partial \bar{y}} \right) (\bar{u} + c) &= -\frac{\partial \bar{p}}{\partial \bar{x}} + \frac{\mu_f}{(1 - \phi)^{2.5}} \left[\frac{\partial^2 \bar{u}}{\partial \bar{x}^2} + \frac{\partial^2 \bar{u}}{\partial \bar{y}^2} \right] \\ &+ g((1 - \phi)\rho_f\beta_f + \phi\rho_p\beta_p) \\ &\times (T - T_0),\end{aligned}\tag{2.28}$$

$$((1 - \phi)\rho_f + \phi\rho_p) \left((\bar{u} + c)\frac{\partial}{\partial \bar{x}} + \bar{v}\frac{\partial}{\partial \bar{y}} \right) \bar{v} = -\frac{\partial \bar{p}}{\partial \bar{y}} + \frac{\mu_f}{(1 - \phi)^{2.5}} \left[\frac{\partial^2 \bar{v}}{\partial \bar{x}^2} + \frac{\partial^2 \bar{v}}{\partial \bar{y}^2} \right],\tag{2.29}$$

$$\begin{aligned}
((1 - \phi)(\rho C)_f + \phi(\rho C)_p) \left((\bar{u} + c) \frac{\partial}{\partial \bar{x}} + \bar{v} \frac{\partial}{\partial \bar{y}} \right) T &= K_f K_1 \left[\frac{\partial^2 T}{\partial \bar{x}^2} + \frac{\partial^2 T}{\partial \bar{y}^2} \right] + \Phi \\
&+ \frac{\mu_f}{(1 - \phi)^{2.5}} \left[2 \left(\left(\frac{\partial \bar{u}}{\partial \bar{x}} \right)^2 + \left(\frac{\partial \bar{v}}{\partial \bar{y}} \right)^2 \right) \right. \\
&\left. + \left(\frac{\partial \bar{u}}{\partial \bar{y}} + \frac{\partial \bar{v}}{\partial \bar{x}} \right)^2 \right]. \tag{2.30}
\end{aligned}$$

2.3.1 Non-dimensionalization

Non-dimensional parameters and variables for the present flow configuration are introduced as follows:

$$\begin{aligned}
x &= \frac{\bar{x}}{\lambda}, \quad y = \frac{\bar{y}}{d}, \quad u = \frac{\bar{u}}{c}, \quad v = \frac{\bar{v}}{c\delta}, \quad \delta = \frac{d}{\lambda}, \quad h = \frac{\bar{H}}{d}, \\
a &= \frac{a_1}{d}, \quad p = \frac{d^2 \bar{p}}{c\lambda\mu_f}, \quad \theta = \frac{T - T_0}{T_0}, \quad \text{Re} = \frac{\rho_f c d}{\mu_f}, \\
\text{Pr} &= \frac{\mu_f C_f}{K_f}, \quad \text{Ec} = \frac{c^2}{C_f T_0}, \quad \text{Br} = \text{Pr Ec}, \quad \varepsilon = \frac{d^2 \Phi}{T_0 K_f}, \\
\text{Gr} &= \frac{g \rho_f \beta_f T_0 d^2}{c \mu_f}, \quad u = \frac{\partial \psi}{\partial y}, \quad v = -\frac{\partial \psi}{\partial x}. \tag{2.31}
\end{aligned}$$

After utilizing the above mentioned non-dimensional quantities we get

$$\delta \text{Re} A_3 \left(\left(\frac{\partial \psi}{\partial y} + 1 \right) \frac{\partial^2 \psi}{\partial y \partial x} - \frac{\partial \psi}{\partial x} \frac{\partial^2 \psi}{\partial y^2} \right) = -\frac{\partial p}{\partial x} + A_1 \left(\delta^2 \frac{\partial^3 \psi}{\partial y \partial x^2} + \frac{\partial^3 \psi}{\partial y^3} \right) + A_2 \text{Gr} \theta, \tag{2.32}$$

$$\delta^3 \text{Re} A_3 \left(-\left(\frac{\partial \psi}{\partial y} + 1 \right) \frac{\partial^2 \psi}{\partial x^2} + \frac{\partial \psi}{\partial x} \frac{\partial^2 \psi}{\partial y \partial x} \right) = -\frac{\partial p}{\partial y} + \delta^2 A_1 \left(-\delta^2 \frac{\partial^3 \psi}{\partial x^3} - \frac{\partial^3 \psi}{\partial y^2 \partial x} \right), \tag{2.33}$$

$$\begin{aligned}
\delta \text{Pr Re} A_4 \left(\left(\frac{\partial \psi}{\partial y} + 1 \right) \frac{\partial \theta}{\partial x} - \frac{\partial \psi}{\partial x} \frac{\partial \theta}{\partial y} \right) &= K_1 \left(\delta^2 \frac{\partial^2 \theta}{\partial x^2} + \frac{\partial^2 \theta}{\partial y^2} \right) + \varepsilon \\
&+ \frac{\text{Br}}{(1 - \phi)^{2.5}} \left[2\delta^2 \left(\left(-\frac{\partial^2 \psi}{\partial y \partial x} \right)^2 + \left(\frac{\partial^2 \psi}{\partial y \partial x} \right)^2 \right) \right. \\
&\left. + \left(-\delta^2 \frac{\partial^2 \psi}{\partial x^2} + \frac{\partial^2 \psi}{\partial y^2} \right)^2 \right] \tag{2.34}
\end{aligned}$$

$$\frac{\partial^2 \psi}{\partial y^2} = 0, \quad \frac{\partial \theta}{\partial y} = 0 \quad \text{at } y = 0, \tag{2.35}$$

$$\frac{\partial \psi}{\partial y} = -1, \quad \theta = 0 \quad \text{at } y = h. \tag{2.36}$$

$$\begin{aligned}
A_1 &= \frac{1}{(1-\phi)^{2.5}}, & A_2 &= 1 - \phi + \phi \left(\frac{(\rho\beta)_p}{(\rho\beta)_f} \right), \\
A_3 &= 1 - \phi + \phi \left(\frac{\rho_p}{\rho_f} \right), & A_4 &= 1 - \phi + \phi \left(\frac{(\rho C)_p}{(\rho C)_f} \right), \\
K_1 &= \frac{K_p + 2K_f - 2\phi(K_f - K_p)}{K_p + 2K_f + \phi(K_f - K_p)} && \text{used for Maxwell's model and} \\
K_1 &= \frac{K_p + (n-1)K_f - (n-1)\phi(K_f - K_p)}{K_p + (n-1)K_f + \phi(K_f - K_p)} && \text{used for Hamilton-Crosser's model(2.37)}
\end{aligned}$$

The wall shape in dimensionless form is

$$h(x) = 1 + a \cos(2\pi x). \quad (2.38)$$

Here δ represents the wave number, a the dimensionless amplitude of peristaltic wave at walls, p represents the dimensionless pressure, Re , Pr , Ec and Br represent the Reynolds, Prandtl, Eckert and Brinkman numbers respectively. ε denotes the heat generation or absorption parameter.

Applying long wavelength and small Reynolds number approximation ultimately Eqs. (2.32)–(2.34) become

$$\frac{\partial p}{\partial x} = A_1 \frac{\partial^3 \psi}{\partial y^3} + A_2 Gr \theta, \quad (2.39)$$

$$\frac{\partial p}{\partial y} = 0, \quad (2.40)$$

$$K_1 \frac{\partial^2 \theta}{\partial y^2} + \frac{Br}{(1-\phi)^{2.5}} \left(\frac{\partial^2 \psi}{\partial y^2} \right)^2 + \varepsilon = 0. \quad (2.41)$$

Dimensionless flow rates in the laboratory $\eta (= \frac{\bar{Q}}{cd})$ and wave frames $F (= \frac{\bar{q}}{cd})$ are related by equation

$$\eta = F + 1, \quad (2.42)$$

where \bar{Q} and \bar{q} represent the dimensional flow rates in the laboratory and wave frames respectively and

$$F = \int_0^h \frac{\partial \psi}{\partial y} dy. \quad (2.43)$$

The boundary conditions in the dimensionless form are defined as

$$\begin{aligned} \psi &= 0, \quad \frac{\partial^2 \psi}{\partial y^2} = 0, \quad \frac{\partial \theta}{\partial y} = 0 \quad \text{at } y = 0, \\ \psi &= F, \quad \frac{\partial \psi}{\partial y} = -1, \quad \theta = 0 \quad \text{at } y = h. \end{aligned} \quad (2.44)$$

Now we cross differentiate the Eqs. (2.39) and (2.40) and get the following Eq.

$$A_1 \frac{\partial^4 \psi}{\partial y^4} + A_2 Gr \frac{\partial \theta}{\partial y} = 0. \quad (2.45)$$

Now we solve the Eqs. (2.41) and (2.45) numerically by NDSolve of MATHEMATICA with boundary conditions given in Eq. (2.44). Results are analyzed physically via graphs.

2.4 Discussion

Via change in nanoparticle volume fraction numerical values for the axial velocity at the center of channel when $Gr = 3.0$, $a = 0.7$, $x = 1$, $\eta = 0.7$, $Br = 0.3$ and $\epsilon = 2.5$.

Table 2.1

Nanoparticles	$\phi = 0.01$	$\phi = 0.01$	$\phi = 0.02$	$\phi = 0.02$
	$U(0)$ for Maxwell	$U(0)$ for H-C	$U(0)$ for Maxwell	$U(0)$ for H-C
TiO ₂	0.822144	0.809994	0.783753	0.762341
Al ₂ O ₃	0.818989	0.800684	0.778032	0.746314
CuO	0.821373	0.8018	0.782426	0.748403
Cu	0.822213	0.801484	0.783979	0.747948
Ag	0.823961	0.80313	0.787197	0.750856
Nanoparticles	$\phi = 0.05$	$\phi = 0.05$	$\phi = 0.1$	$\phi = 0.1$
	$U(0)$ for Maxwell	$U(0)$ for H-C	$U(0)$ for Maxwell	$U(0)$ for H-C
TiO ₂	0.685082	0.647393	0.561421	0.516771
Al ₂ O ₃	0.674205	0.620556	0.547001	0.486308
CuO	0.682959	0.624876	0.559468	0.492701
Cu	0.686085	0.624521	0.56397	0.492973
Ag	0.692459	0.629783	0.572938	0.499696

Via change in nanoparticle volume fraction numerical values for the temperature at the center of channel when $Gr = 3.0, a = 0.7, x = 1, \eta = 0.7, Br = 0.3$ and $\epsilon = 2.5$.

Table 2.2

Nanoparticles	$\phi = 0.01$	$\phi = 0.01$	$\phi = 0.02$	$\phi = 0.02$
	$\theta(0)$ for Maxwell	$\theta(0)$ for H-C	$\theta(0)$ for Maxwell	$\theta(0)$ for H-C
TiO ₂	4.2984	4.20839	4.15376	3.98999
Al ₂ O ₃	4.27595	4.14036	4.11178	3.86923
CuO	4.27713	4.13269	4.11343	3.85522
Cu	4.27606	4.12336	4.1112	3.83866
Ag	4.27885	4.12574	4.11608	3.84245
Nanoparticles	$\phi = 0.05$	$\phi = 0.05$	$\phi = 0.1$	$\phi = 0.1$
	$\theta(0)$ for Maxwell	$\theta(0)$ for H-C	$\theta(0)$ for Maxwell	$\theta(0)$ for H-C
TiO ₂	3.77532	3.45692	3.27644	2.82643
Al ₂ O ₃	3.68751	3.23417	3.13838	2.52572
CuO	3.68803	3.20668	3.13367	2.48647
Cu	3.6821	3.17624	3.12201	2.44574
Ag	3.6905	3.18144	3.13169	2.45034

In this section analysis of obtained numerical results is done. Our main focus is to compare the results obtained in the case of two thermal conductivity models i.e. Maxwell and Hamilton-Crosser. Moreover analysis is also done using five different nanofluids. For the sake of comparison of effective thermal conductivity between two phase models (Maxwell and Hamilton-Crosser) and by using different nanoparticles *Fig. 2.2* is plotted. It is observed through the figure that effective thermal conductivity estimated through the Hamilton-Crosser model is greater than the Maxwell model. Moreover the difference in value of effective thermal conductivity become larger when the nanoparticle volume fraction become enlarge. Also, this difference between the values of effective thermal conductivity of two models become larger when the nanoparticle with high thermal conductivity are utilized.

2.4.1 Analysis of velocity profile

In this subsection examination of numerical values for axial velocity at the channel's center is done. The values of axial velocity at the center of the channel for the case of both effective thermal conductivity models are presented through the Table 2.1. Observations show that the axial velocity at the center of the channel is greater for Maxwell model than Hamilton-Crosser model in all the cases when the nanoparticle volume fraction varies. Moreover when the metallic nanoparticles are used, the difference between the values obtained by two models become larger than the metallic oxides nanoparticles. Furthermore such difference is also larger when nanoparticles volume fraction get larger values.

2.4.2 Analysis of temperature profile

The temperature profile at the center of channel is analyzed through the numerical data given in Table 2.2. It is examined through the table that the temperature profile at the center of the channel shows less values in the case of Hamilton-Crosser model as compared to that of Maxwell model. It is also noticed that when we increase the volume fraction of the nanoparticles in the nanofluid the difference between the values estimated by utilizing the two thermal conductivity models become large. Moreover for metallic particles the difference between estimated values of two models is larger than the metallic oxides ones.

2.4.3 Heat transfer rate

To see the behavior of nanoparticles volume fraction on the heat transfer rate at the wall for five different type of nanoparticles used in the analysis *Figs. 2.3 – 2.7* are drawn. These figures also give the comparison of the values estimated by the two thermal conductivity models. The row of the bars present the value predicted by the Maxwell model of thermal conductivity whereas the second row of the bars represent the values for Hamilton-Crosser model. It is examined through these graphs that the heat transfer rate at the wall predicted by Hamilton-Crosser model is greater than Maxwell model for all the nanoparticles used in the analysis. It is also noticed that heat transfer rate at the wall increases when volume fraction of the nanoparticles enlarged. Also heat transfer rate is higher for the nanoparticle with high thermal conductivity. The difference between the values of the two model increases when nanoparticle volume fraction is enhanced.

This difference also increases when nanoparticles with greater thermal conductivity value is used.

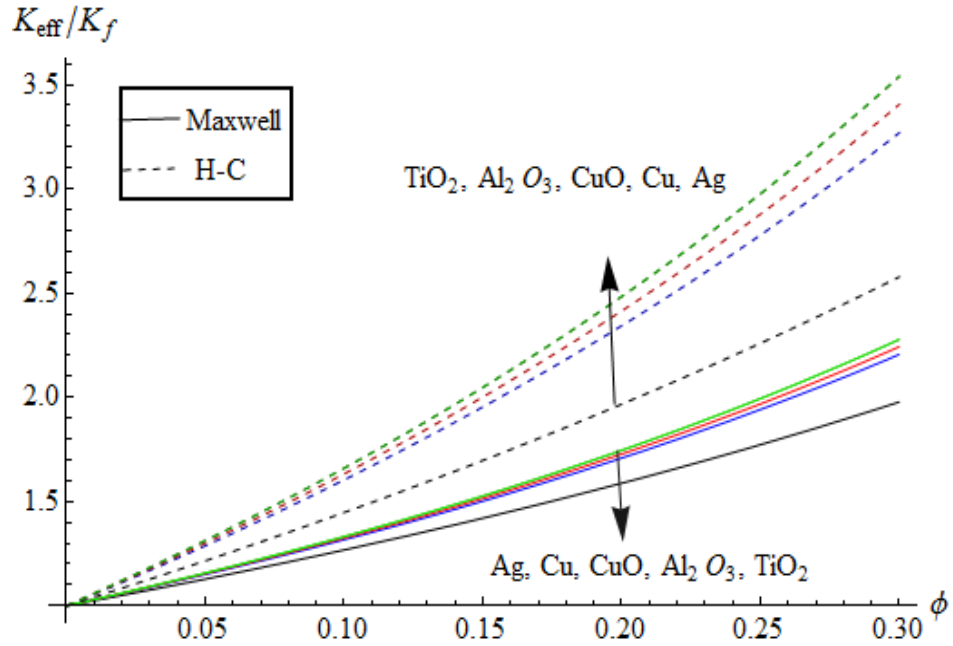


Fig. 2.2. Effective thermal conductivity for Maxwell's and Hamilton-Crosser's model

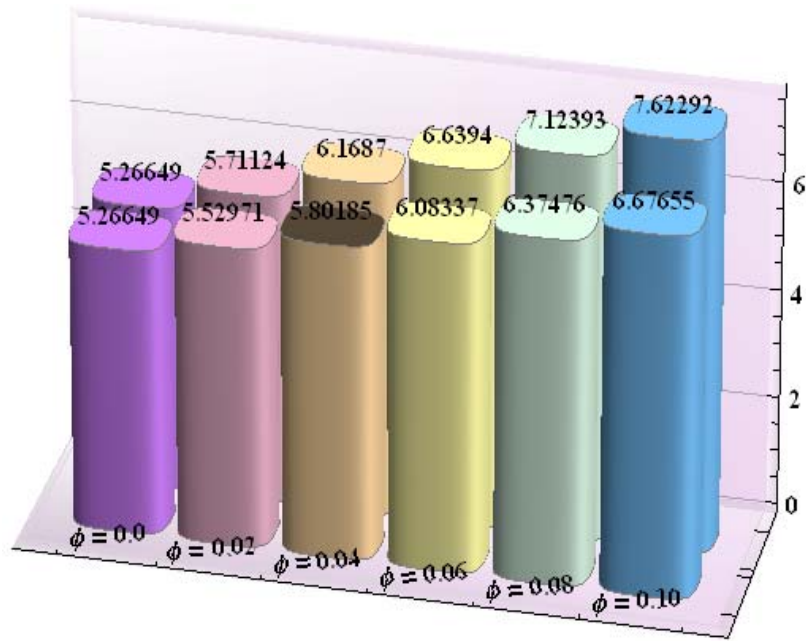


Fig. 2.3. Change via nanoparticle volume fraction in heat transfer rate at the wall ($-\frac{K_{eff}}{K_f} \theta'(h)$) for TiO_2 -water nanofluid when $Gr = 3.0$, $a = 0.7$, $x = 0$, $\eta = 0.7$, $Br = 0.3$ and $\epsilon = 2.5$.

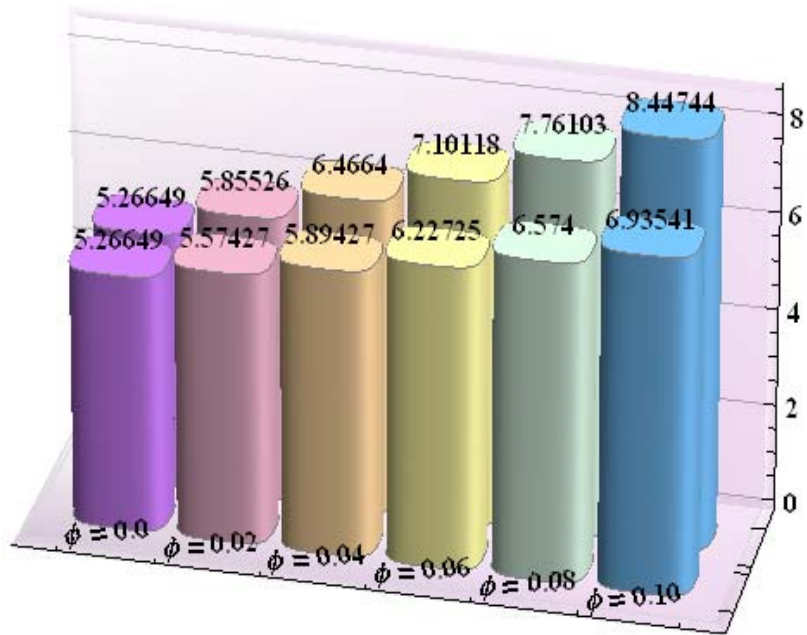


Fig. 2.4. Change via nanoparticle volume fraction in heat transfer rate at the wall ($-\frac{K_{eff}}{K_f} \theta'(h)$) for Al_2O_3 -water nanofluid when $Gr = 3.0$, $a = 0.7$, $x = 0$, $\eta = 0.7$, $Br = 0.3$ and $\epsilon = 2.5$.

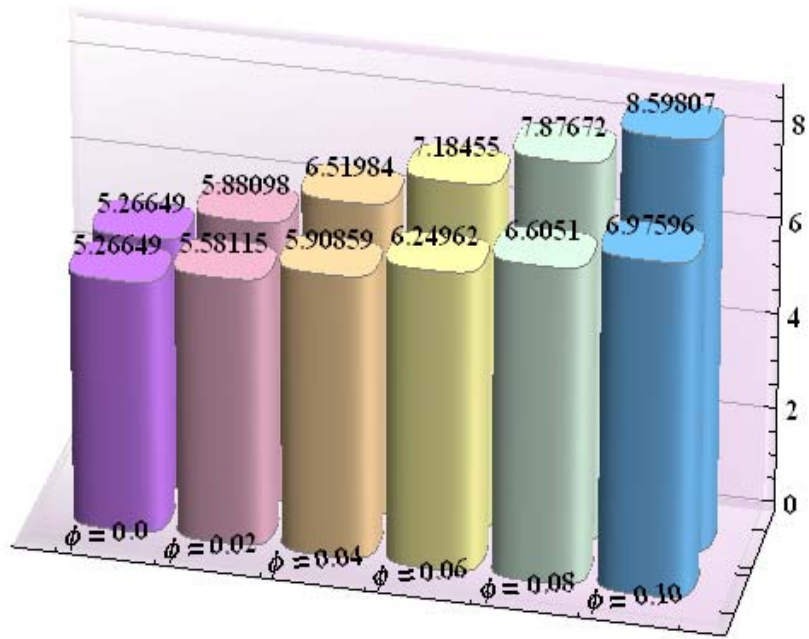


Fig. 2.5. Change via nanoparticle volume fraction in heat transfer rate at the wall ($-\frac{K_{eff}}{K_f} \theta'(h)$) for *CuO*-water nanofluid when $Gr = 3.0$, $a = 0.7$, $x = 0$, $\eta = 0.7$, $Br = 0.3$ and $\epsilon = 2.5$.

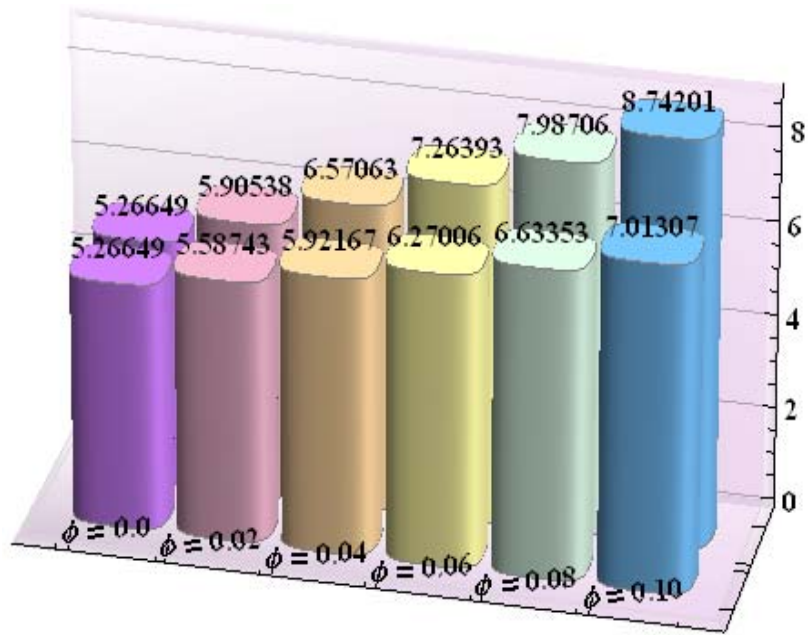


Fig. 2.6. Change via nanoparticle volume fraction in heat transfer rate at the wall ($-\frac{K_{eff}}{K_f} \theta'(h)$) for Cu -water nanofluid when $Gr = 3.0$, $a = 0.7$, $x = 0$, $\eta = 0.7$, $Br = 0.3$ and $\epsilon = 2.5$.

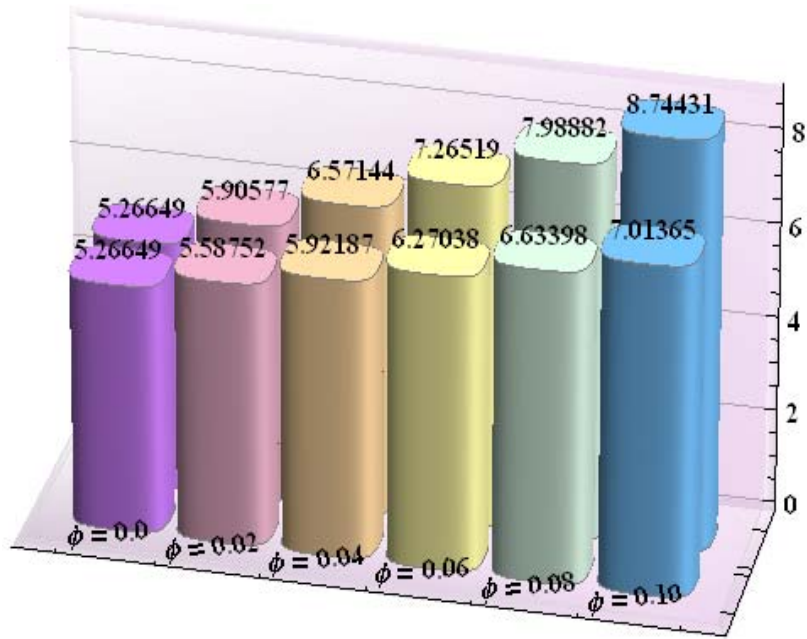


Fig. 2.7. Change via nanoparticle volume fraction in heat transfer rate at the wall ($-\frac{K_{eff}}{K_f} \theta'(h)$) for Ag-water nanofluid when $Gr = 3.0$, $a = 0.7$, $x = 0$, $\eta = 0.7$, $Br = 0.3$ and $\epsilon = 2.5$.

Chapter 3

A model for an application to biomedical engineering through nanoparticles

3.1 Introduction

Main purpose of this chapter is to analyze partial slip conditions on the mixed convective peristaltic flow of water based nanofluids in a vertical asymmetric channel. Viscous dissipation and heat generation/absorption effects are present. Problem is solved by utilizing the lubrication technique. Five types of nanofluids are utilized in the analysis comprising of nanoparticles namely Titanium oxide or titania (TiO_2), Aluminum oxide or Alumina (Al_2O_3), Copper oxide (CuO), Copper (Cu) and Silver (Ag) with water as base fluid. Study is based on the comparison of two effective thermal conductivity models namely as Maxwell model of thermal conductivity and Hamilton-Crosser model of thermal conductivity. Effects of slip parameters on the axial velocity and temperature are examined for all the nanofluids considered in the problem. Further the impact of nanoparticle volume fraction on the axial velocity profile, temperature distribution and heat transfer rate at the wall is analyzed for the two thermal conductivity models. Further NDSolve is employed for the computations.

3.2 Mathematical formulation

We examine the two dimensional flow of an incompressible nanofluid in an asymmetric vertical channel of width $d_1 + d_2$. Two sinusoidal waves of speed c having the small amplitudes a_1 and b_1 with wavelength λ induces the flow in channel (*see Fig. 3.1*). The shapes of the walls are given by the expression defined below:

$$\bar{Y} = \bar{H}_1(\bar{X}, \bar{t}) = d_1 + a_1 \cos \frac{2\pi}{\lambda} (\bar{X} - c\bar{t}), \quad \text{at right wall,} \quad (3.1)$$

$$\bar{Y} = \bar{H}_2(\bar{X}, \bar{t}) = -d_2 - b_1 \cos \left(\frac{2\pi}{\lambda} (\bar{X} - c\bar{t}) + \gamma \right), \quad \text{at left wall.} \quad (3.2)$$

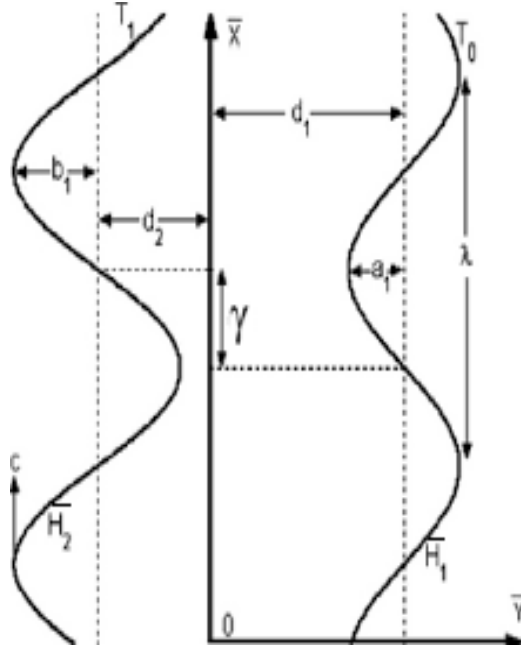


Fig. 3.1: Schematic diagram

Here the walls of the channel $\bar{H}_1(\bar{X}, \bar{t})$ and $\bar{H}_2(\bar{X}, \bar{t})$ are in the region $\bar{Y} > 0$ and $\bar{Y} < 0$ with amplitudes a_1 and b_1 respectively. The phase difference between the two waves is depicted by the notation γ whose range varies between $0 \leq \gamma \leq \pi$ and \bar{t} is use for the time. Moreover following condition must satisfy by a_1 , b_1 , d_1 , d_2 and γ

$$a_1^2 + b_1^2 + 2a_1b_1 \cos \gamma \leq (d_1 + d_2)^2.$$

The constant temperature T_0 and T_1 ($> T_0$) are maintained at the respective walls $\overline{H}_1(\overline{X}, \overline{t})$ and $\overline{H}_2(\overline{X}, \overline{t})$. The velocity field for the two dimensional flow configuration is represented by $[\overline{U}(\overline{X}, \overline{Y}, \overline{t}), \overline{V}(\overline{X}, \overline{Y}, \overline{t}), 0]$.

The governing system of equations for the considered flow is

$$\frac{\partial \overline{U}}{\partial \overline{X}} + \frac{\partial \overline{V}}{\partial \overline{Y}} = 0, \quad (3.3)$$

$$\rho_{eff} \left(\frac{\partial}{\partial \overline{t}} + \overline{U} \frac{\partial}{\partial \overline{X}} + \overline{V} \frac{\partial}{\partial \overline{Y}} \right) \overline{U} = -\frac{\partial \overline{P}}{\partial \overline{X}} + \mu_{eff} \left[\frac{\partial^2 \overline{U}}{\partial \overline{X}^2} + \frac{\partial^2 \overline{U}}{\partial \overline{Y}^2} \right] + g(\rho\beta)_{eff} (T - T_m), \quad (3.4)$$

$$\rho_{eff} \left(\frac{\partial}{\partial \overline{t}} + \overline{U} \frac{\partial}{\partial \overline{X}} + \overline{V} \frac{\partial}{\partial \overline{Y}} \right) \overline{V} = -\frac{\partial \overline{P}}{\partial \overline{Y}} + \mu_{eff} \left[\frac{\partial^2 \overline{V}}{\partial \overline{X}^2} + \frac{\partial^2 \overline{V}}{\partial \overline{Y}^2} \right], \quad (3.5)$$

$$\begin{aligned} (\rho C)_{eff} \left(\frac{\partial}{\partial \overline{t}} + \overline{U} \frac{\partial}{\partial \overline{X}} + \overline{V} \frac{\partial}{\partial \overline{Y}} \right) T &= K_{eff} \left[\frac{\partial^2 T}{\partial \overline{X}^2} + \frac{\partial^2 T}{\partial \overline{Y}^2} \right] + \Phi \\ &+ \mu_{eff} \left[2 \left(\left(\frac{\partial \overline{U}}{\partial \overline{X}} \right)^2 + \left(\frac{\partial \overline{V}}{\partial \overline{Y}} \right)^2 \right) \right. \\ &\left. + \left(\frac{\partial \overline{U}}{\partial \overline{Y}} + \frac{\partial \overline{V}}{\partial \overline{X}} \right)^2 \right]. \end{aligned} \quad (3.6)$$

The slip conditions at the walls in the fixed frame of reference are given by

$$\begin{aligned} \overline{U}_w - \overline{U}(\overline{X}, \overline{H}_1, \overline{t}) &= \tilde{n} * \xi_1 * \tau_{xy}, \quad \text{at } \overline{Y} = \overline{H}_1, \\ \overline{U}(\overline{X}, \overline{H}_2, \overline{t}) - \overline{U}_w &= \tilde{n} * \xi_1 * \tau_{xy}, \quad \text{at } \overline{Y} = \overline{H}_2, \end{aligned} \quad (3.7)$$

$$\begin{aligned} T - T_w + \tilde{n} * \zeta_1 * \frac{\partial T}{\partial \overline{Y}} &= 0 \quad \text{at } \overline{Y} = \overline{H}_1, \\ T - T_w - \tilde{n} * \zeta_1 * \frac{\partial T}{\partial \overline{Y}} &= 0 \quad \text{at } \overline{Y} = \overline{H}_2, \end{aligned} \quad (3.8)$$

where \overline{U}_w and T_w represent the velocity and temperature at the wall respectively. Shear stress is represented by τ_{xy} whereas the dimensional form of slip parameters for the velocity and temperature are denoted by ξ_1 and ζ_1 respectively.

The transformation between fixed and moving frame of reference is given by

$$\begin{aligned}\bar{x} &= \bar{X} - c\bar{t}, \quad \bar{y} = \bar{Y}, \quad \bar{u}(\bar{x}, \bar{y}) = \bar{U}(\bar{X}, \bar{Y}, \bar{t}) - c, \\ \bar{v}(\bar{x}, \bar{y}) &= \bar{V}(\bar{X}, \bar{Y}, \bar{t}), \quad \bar{p}(\bar{x}, \bar{y}) = \bar{P}(\bar{X}, \bar{Y}, \bar{t}).\end{aligned}\quad (3.9)$$

Applying these transformation our system of equations and boundary conditions become

$$\frac{\partial \bar{u}}{\partial \bar{x}} + \frac{\partial \bar{v}}{\partial \bar{y}} = 0, \quad (3.10)$$

$$\begin{aligned}((1 - \phi)\rho_f + \phi\rho_p) \left((\bar{u} + c) \frac{\partial}{\partial \bar{x}} + \bar{v} \frac{\partial}{\partial \bar{y}} \right) (\bar{u} + c) &= -\frac{\partial \bar{p}}{\partial \bar{x}} + \frac{\mu_f}{(1 - \phi)^{2.5}} \left[\frac{\partial^2 \bar{u}}{\partial \bar{x}^2} + \frac{\partial^2 \bar{u}}{\partial \bar{y}^2} \right] \\ &+ g((1 - \phi)\rho_f \beta_f + \phi\rho_p \beta_p) \\ &\times (T - T_m),\end{aligned}\quad (3.11)$$

$$((1 - \phi)\rho_f + \phi\rho_p) \left((\bar{u} + c) \frac{\partial}{\partial \bar{x}} + \bar{v} \frac{\partial}{\partial \bar{y}} \right) \bar{v} = -\frac{\partial \bar{p}}{\partial \bar{y}} + \frac{\mu_f}{(1 - \phi)^{2.5}} \left[\frac{\partial^2 \bar{v}}{\partial \bar{x}^2} + \frac{\partial^2 \bar{v}}{\partial \bar{y}^2} \right], \quad (3.12)$$

$$\begin{aligned}((1 - \phi)(\rho C)_f + \phi(\rho C)_p) \left((\bar{u} + c) \frac{\partial}{\partial \bar{x}} + \bar{v} \frac{\partial}{\partial \bar{y}} \right) T &= K_f K_1 \left[\frac{\partial^2 T}{\partial \bar{x}^2} + \frac{\partial^2 T}{\partial \bar{y}^2} \right] + \Phi + \\ &\frac{\mu_f}{(1 - \phi)^{2.5}} \left[2 \left(\left(\frac{\partial \bar{u}}{\partial \bar{x}} \right)^2 + \left(\frac{\partial \bar{v}}{\partial \bar{y}} \right)^2 \right) \right. \\ &\left. + \left(\frac{\partial \bar{u}}{\partial \bar{y}} + \frac{\partial \bar{v}}{\partial \bar{x}} \right)^2 \right].\end{aligned}\quad (3.13)$$

$$\begin{aligned}u(\bar{x}, \bar{h}_1) + c + \tilde{n} * \xi_1 * \tau_{xy} &= 0, \quad \text{at } \bar{y} = \bar{h}_1, \\ u(\bar{x}, \bar{h}_2) + c - \tilde{n} * \xi_1 * \tau_{xy} &= 0, \quad \text{at } \bar{y} = \bar{h}_2,\end{aligned}\quad (3.14)$$

$$T + \tilde{n} * \zeta_1 * \frac{\partial T}{\partial \bar{y}} = T_0 \quad \text{at } \bar{y} = \bar{h}_1, \quad (3.15)$$

$$T - \tilde{n} * \zeta_1 * \frac{\partial T}{\partial \bar{y}} = T_1 \quad \text{at } \bar{y} = \bar{h}_2. \quad (3.16)$$

Dimensionless form of variables and parameters are defined as

$$\begin{aligned}
x &= \frac{\bar{x}}{\lambda}, & y &= \frac{\bar{y}}{d_1}, & u &= \frac{\bar{u}}{c}, & v &= \frac{\bar{v}}{c\delta}, & \delta &= \frac{d_1}{\lambda}, & h_1 &= \frac{\bar{H}_1}{d_1}, & h_2 &= \frac{\bar{H}_2}{d_1}, \\
d &= \frac{d_2}{d_1}, & a &= \frac{a_1}{d_1}, & b &= \frac{b_1}{d_1}, & p &= \frac{d_1^2 \bar{p}}{c\lambda\mu_f}, & \theta &= \frac{T - T_m}{T_1 - T_0}, & \text{Re} &= \frac{\rho_f c d_1}{\mu_f}, \\
\text{Pr} &= \frac{\mu_f C_f}{K_f}, & Ec &= \frac{c^2}{C_f(T_1 - T_0)}, & Br &= \text{Pr} Ec, & \varepsilon &= \frac{d_1^2 \Phi}{(T_1 - T_0)K_f}, & \zeta &= \frac{\zeta_1}{d_1}, \\
\xi &= \frac{\xi_1 \mu_f}{d_1}, & Gr &= \frac{g\rho_f \beta_f (T_1 - T_0) d_1^2}{c\mu_f}, & u &= \frac{\partial \psi}{\partial y}, & v &= -\frac{\partial \psi}{\partial x}.
\end{aligned} \tag{3.17}$$

Here δ represents the wave number, a and b are the dimensionless amplitudes of peristaltic wave at walls, T_m ($= \frac{T_1 + T_0}{2}$) is the mean temperature, p represents the dimensionless pressure, Re , Pr , Ec and Br represent the Reynolds, Prandtl, Eckert and Brinkman numbers respectively. ε denotes the heat generation or absorption parameter. Moreover dimensionless slip parameters for velocity and temperature are defined by ξ and ζ respectively.

Using non-dimensional variables, the governing mathematical problem is

$$\delta \text{Re} A_3 \left(\left(\frac{\partial \psi}{\partial y} + 1 \right) \frac{\partial^2 \psi}{\partial y \partial x} - \frac{\partial \psi}{\partial x} \frac{\partial^2 \psi}{\partial y^2} \right) = -\frac{\partial p}{\partial x} + A_1 \left(\delta^2 \frac{\partial^3 \psi}{\partial y \partial x^2} + \frac{\partial^3 \psi}{\partial y^3} \right) + A_2 Gr \theta, \tag{3.18}$$

$$\delta^3 \text{Re} A_3 \left(-\left(\frac{\partial \psi}{\partial y} + 1 \right) \frac{\partial^2 \psi}{\partial x^2} + \frac{\partial \psi}{\partial x} \frac{\partial^2 \psi}{\partial y \partial x} \right) = -\frac{\partial p}{\partial y} + \delta^2 A_1 \left(-\delta^2 \frac{\partial^3 \psi}{\partial x^3} - \frac{\partial^3 \psi}{\partial y^2 \partial x} \right), \tag{3.19}$$

$$\begin{aligned}
\delta \text{Pr} \text{Re} A_4 \left(\left(\frac{\partial \psi}{\partial y} + 1 \right) \frac{\partial \theta}{\partial x} - \frac{\partial \psi}{\partial x} \frac{\partial \theta}{\partial y} \right) &= K_1 \left(\delta^2 \frac{\partial^2 \theta}{\partial x^2} + \frac{\partial^2 \theta}{\partial y^2} \right) + \varepsilon \\
&+ \frac{Br}{(1 - \phi)^{2.5}} \left[\begin{aligned} &2\delta^2 \left(\left(-\frac{\partial^2 \psi}{\partial y \partial x} \right)^2 + \left(\frac{\partial^2 \psi}{\partial y \partial x} \right)^2 \right) \\ &+ \left(-\delta^2 \frac{\partial^2 \psi}{\partial x^2} + \frac{\partial^2 \psi}{\partial y^2} \right)^2 \end{aligned} \right] \tag{3.20}
\end{aligned}$$

$$\begin{aligned}
A_1 &= \frac{1}{(1-\phi)^{2.5}}, \quad A_2 = 1 - \phi + \phi \left(\frac{(\rho\beta)_p}{(\rho\beta)_f} \right), \\
A_3 &= 1 - \phi + \phi \left(\frac{\rho_p}{\rho_f} \right), \quad A_4 = 1 - \phi + \phi \left(\frac{(\rho C)_p}{(\rho C)_f} \right), \\
K_1 &= \frac{K_p + 2K_f - 2\phi(K_f - K_p)}{K_p + 2K_f + \phi(K_f - K_p)} \quad \text{used for Maxwell's model and} \\
K_1 &= \frac{K_p + (n-1)K_f - (n-1)\phi(K_f - K_p)}{K_p + (n-1)K_f + \phi(K_f - K_p)} \quad \text{used for Hamilton-Crosser's model(3.21)}
\end{aligned}$$

Flow rates in the laboratory $\eta(= \frac{\bar{Q}}{cd_1})$ and wave frames $F(= \frac{\bar{q}}{cd_1})$ in non-dimensional form are corelated by equation

$$\eta = F + 1 + d, \quad (3.22)$$

where \bar{Q} and \bar{q} show the dimensional flow rates in the laboratory and wave frames respectively and

$$F = \int_{h_2}^{h_1} \frac{\partial \psi}{\partial y} dy. \quad (3.23)$$

The dimensionless form of considered boundary conditions become

$$\begin{aligned}
\psi &= \frac{F}{2}, \quad \frac{\partial \psi}{\partial y} + \frac{\xi}{(1-\phi)^{2.5}} \frac{\partial^2 \psi}{\partial y^2} = -1, \quad \theta + \zeta \frac{\partial \theta}{\partial y} = -\frac{1}{2}, \quad \text{at } y = h_1, \\
\psi &= -\frac{F}{2}, \quad \frac{\partial \psi}{\partial y} - \frac{\xi}{(1-\phi)^{2.5}} \frac{\partial^2 \psi}{\partial y^2} = -1, \quad \theta - \zeta \frac{\partial \theta}{\partial y} = \frac{1}{2}, \quad \text{at } y = h_2,
\end{aligned} \quad (3.24)$$

where the dimensionless form of walls are written as

$$\begin{aligned}
h_1(x) &= 1 + a \cos(2\pi x), \\
h_2(x) &= -d - b \cos(2\pi x + \gamma).
\end{aligned} \quad (3.25)$$

In view of lubrication approach our system of Eqs. and boundary conditions become

$$\frac{\partial p}{\partial x} = A_1 \frac{\partial^3 \psi}{\partial y^3} + A_2 Gr \theta, \quad (3.26)$$

$$\frac{\partial p}{\partial y} = 0, \quad (3.27)$$

$$K_1 \frac{\partial^2 \theta}{\partial y^2} + \frac{Br}{(1-\phi)^{2.5}} \left(\frac{\partial^2 \psi}{\partial y^2} \right)^2 + \varepsilon = 0, \quad (3.28)$$

$$\begin{aligned} \psi &= \frac{F}{2}, \quad \frac{\partial \psi}{\partial y} + \frac{\xi}{(1-\phi)^{2.5}} \frac{\partial^2 \psi}{\partial y^2} = -1, \quad \theta + \zeta \frac{\partial \theta}{\partial y} = -\frac{1}{2}, \quad \text{at } y = h_1, \\ \psi &= -\frac{F}{2}, \quad \frac{\partial \psi}{\partial y} - \frac{\xi}{(1-\phi)^{2.5}} \frac{\partial^2 \psi}{\partial y^2} = -1, \quad \theta - \zeta \frac{\partial \theta}{\partial y} = \frac{1}{2}, \quad \text{at } y = h_2. \end{aligned} \quad (3.29)$$

The above mentioned system with the corresponding boundary conditions in Eq. (3.29) are solved numerically with the help of NDSolve of MATHEMATICA.

3.3 Analysis and discussion

This section is prepared to examine the effects of different embedded parameters on the axial velocity, temperature and heat transfer rate at the wall. Analysis include the comparison of axial velocity profile, temperature distribution and heat transfer rate at the wall for the case of considered two effective thermal conductivity models.

Fig. 3.2 is plotted to observe the comparison of the effective thermal conductivity of the nanofluids estimated by the Maxwell's and Hamilton-Crosser's models. It is observed from Fig. that the effective thermal conductivity anticipated by Hamilton-Crosser's model is greater than the Maxwell's model for all nanoparticles used. Likewise by increasing the nanoparticle volume fraction the difference between the effective thermal conductivity predicted by the two models became large. For metallic particles such difference is greater than the metallic oxides nanoparticles.

Figs. (3.3-3.7) depict the velocity profile for five different nanoparticles (TiO₂, Al₂O₃, CuO, Cu, Ag), for two considered model i-e Maxwell's and Hamilton-Crosser's. It can be seen from Figs. that the axial velocity is maximum near the center of the channel. It can also be observed that value of axial velocity decreases by enhancing the volume fraction of nanoparticles. The fact behind this behavior is that by increasing the nanoparticles volume fraction the resistance to the flow increases and the fluid can not attain the high values of velocity. It is illustrated by the Figs. that the values of axial velocity near the center of channel is higher for Maxwell's thermal conductivity model in comparison to Hamilton-Crosser's thermal conductivity model.

This difference is enhanced as we increase the volume fraction of nanoparticles. Moreover for the nanoparticles with high thermal conductivities like metallic particles such difference enhances.

Figs. (3.8-3.12) elucidate the velocity profile for five nanofluids while velocity slip parameter is varying. It can be examined that with an increase in the velocity slip parameter the maximum velocity of the nanofluid decreases.

Figs. (3.13-3.17) illustrate the behavior of temperature profile for different nanoparticles when their volume fraction ϕ is varying. The results are discussed for Hamilton-Crosser's and Maxwell's model. It can be noticed that the values of temperature decreases with an increase in nanoparticles volume fraction. The reason of decreasing the temperature profile is the high thermal conductivity of the nanoparticles which enhanced the heat transfer rate, as a result temperature decreases. Moreover the values of temperature for Maxwell's thermal conductivity model is higher than the Hamilton-Crosser's model in all cases. It is concluded from the results that with enhancement in nanoparticles volume fraction such difference widens. Also by using the nanoparticles with high thermal conductivities the difference between the two models became large.

Figs. (3.18-3.22) show the effect of thermal slip parameter on temperature. Clearly it can be seen that with an increase in the thermal slip parameter temperature of the fluid increases uniformly throughout the channel. Physically the thermal slip parameter appear because of the difference in the temperature of the boundary and the fluid near at the interface.

Figs.(3.23-3.27) are sketched to examine the heat transfer rate at the wall for different nanoparticles by altering the nanoparticle volume fraction for two effective thermal conductivity models (i-e Maxwell's and H-C's). The front row of the bars represents the values of heat transfer rate at the wall for Maxwell's model whereas the back row is for the heat transfer rate at the wall for Hamilton-Crosser's model. It is examined from the Figs. that the heat transfer rate at the wall enhances by increasing the volume fraction of nanoparticles.

Furthermore, it is observed that the values of Hamilton-Crosser's model is greater than the values of Maxwell's model. So we concluded that the difference in the values of Maxwell's and Hamilton-Crosser's model increases by increase in nanoparticles volume fraction and heat transfer rate is higher for the nanoparticle with high thermal conductivity.

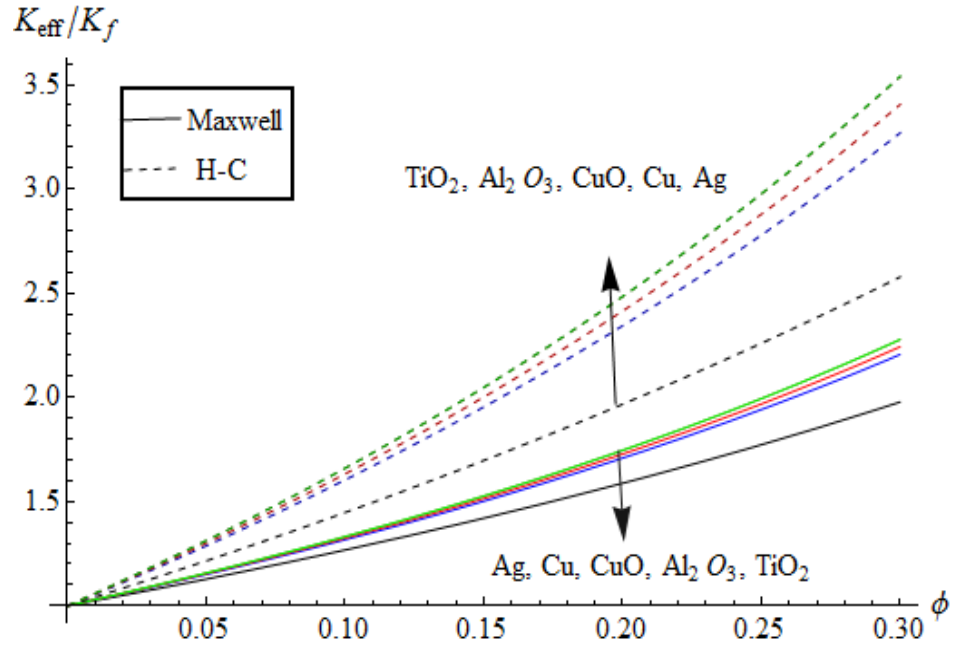


Fig. 3.2. Effective thermal conductivity for Maxwell's and Hamilton-Crosser's model

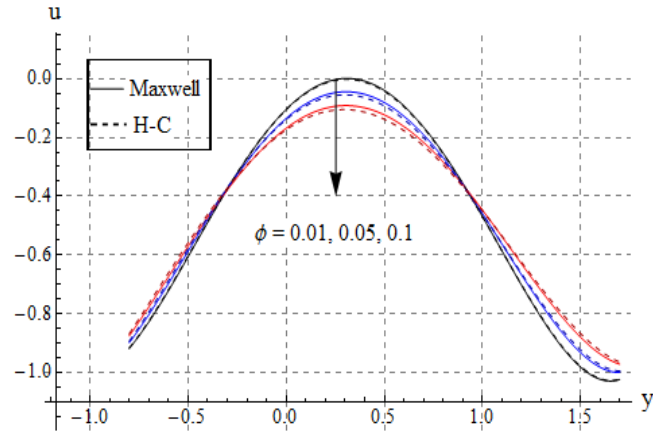


Fig. 3.3. Variation of axial velocity for TiO_2 for change in ϕ when $a = 0.7$, $b = 0.6$, $\gamma = \pi/2$, $d = 0.8$, $x = 0$, $\eta = 0.7$, $Br = 0.3$, $\xi = 0.1$, $\zeta = 0.1$, $Gr = 3.0$, $\epsilon = 2.5$.

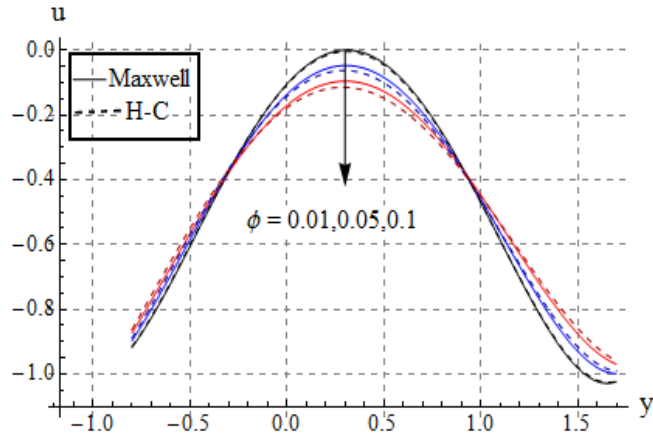


Fig. 3.4. Variation of axial velocity for Al_2O_3 for change in ϕ when $a = 0.7$, $b = 0.6$, $\gamma = \pi/2$, $d = 0.8$, $x = 0$, $\eta = 0.7$, $Br = 0.3$, $\xi = 0.1$, $\zeta = 0.1$, $Gr = 3.0$, $\epsilon = 2.5$.

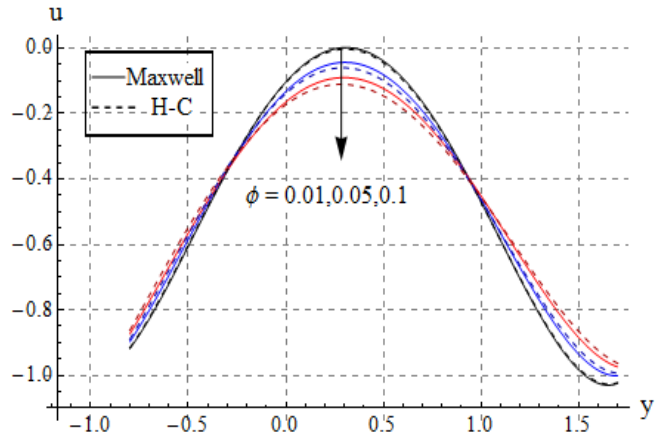


Fig. 3.5. Variation of axial velocity for CuO for change in ϕ when $a = 0.7$, $b = 0.6$, $\gamma = \pi/2$, $d = 0.8$, $x = 0$, $\eta = 0.7$, $Br = 0.3$, $\xi = 0.1$, $\zeta = 0.1$, $Gr = 3.0$, $\epsilon = 2.5$.

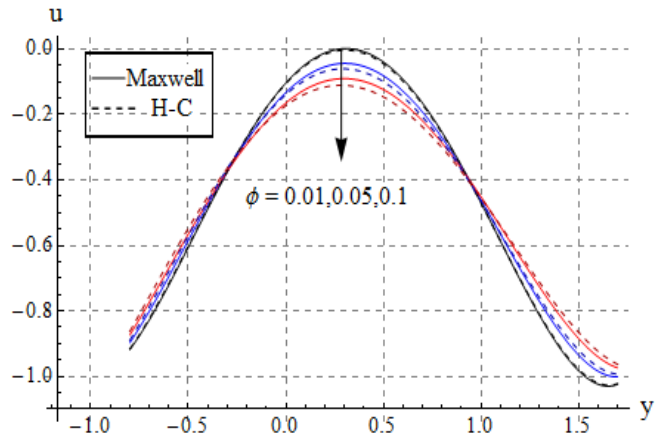


Fig. 3.6. Variation of axial velocity for Cu for change in ϕ when $a = 0.7$, $b = 0.6$, $\gamma = \pi/2$, $d = 0.8$, $x = 0$, $\eta = 0.7$, $Br = 0.3$, $\xi = 0.1$, $\zeta = 0.1$, $Gr = 3.0$, $\epsilon = 2.5$.

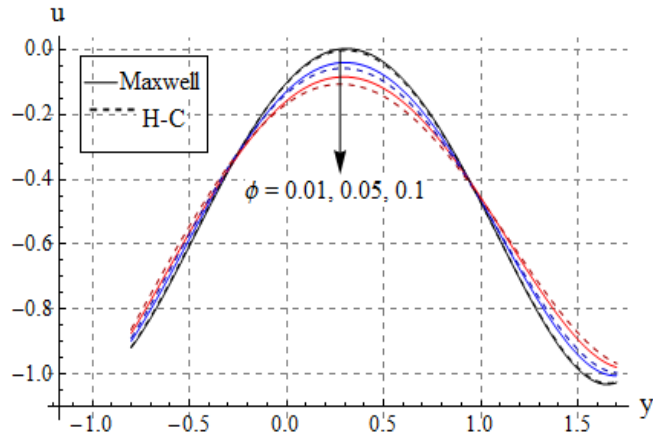


Fig. 3.7. Variation of axial velocity for Ag for change in ϕ when $a = 0.7$, $b = 0.6$, $\gamma = \pi/2$, $d = 0.8$, $x = 0$, $\eta = 0.7$, $Br = 0.3$, $\xi = 0.1$, $\zeta = 0.1$, $Gr = 3.0$, $\epsilon = 2.5$.

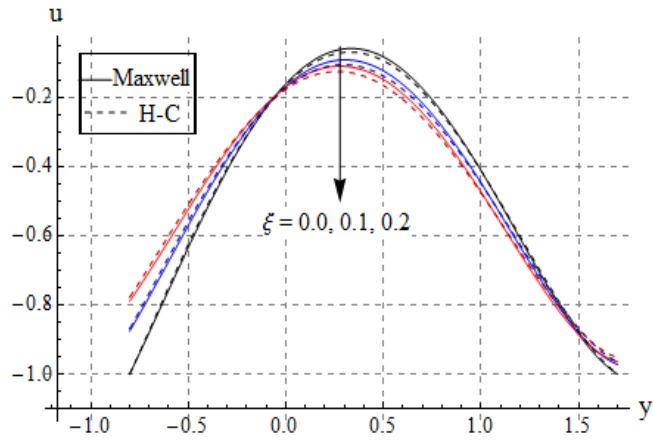


Fig. 3.8. Variation of velocity for TiO_2 for change in velocity slip when $a = 0.7$, $b = 0.6$, $\gamma = \pi/2$, $d = 0.8$, $x = 0$, $\eta = 0.7$, $Br = 0.3$, $\zeta = 0.1$, $\phi = 0.1$, $Gr = 3.0$, $\epsilon = 2.5$.

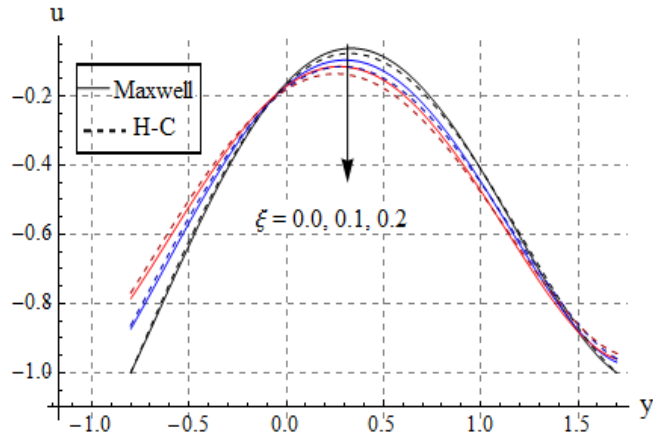


Fig. 3.9. Variation of velocity for Al_2O_3 for change in velocity slip when $a = 0.7$, $b = 0.6$, $\gamma = \pi/2$, $d = 0.8$, $x = 0$, $\eta = 0.7$, $Br = 0.3$, $\zeta = 0.1$, $\phi = 0.1$, $Gr = 3.0$, $\epsilon = 2.5$.

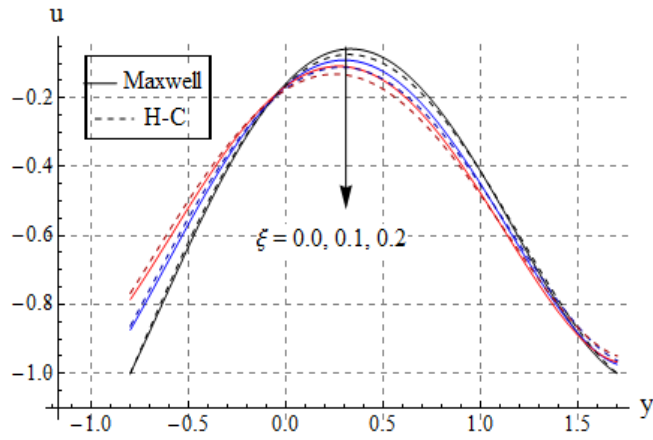


Fig. 3.10. Variation of velocity for CuO for change in velocity when $a = 0.7$, $b = 0.6$, $\gamma = \pi/2$, $d = 0.8$, $x = 0$, $\eta = 0.7$, $Br = 0.3$, $\zeta = 0.1$, $\phi = 0.1$, $Gr = 3.0$, $\epsilon = 2.5$.

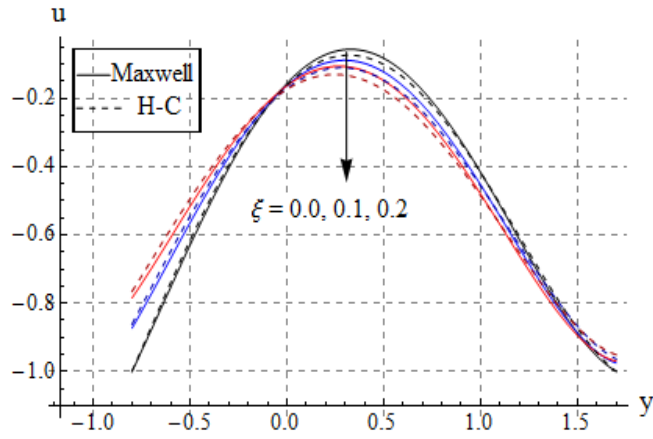


Fig. 3.11. Variation of velocity for Cu for change in velocity slip when $a = 0.7$, $b = 0.6$, $\gamma = \pi/2$, $d = 0.8$, $x = 0$, $\eta = 0.7$, $Br = 0.3$, $\zeta = 0.1$, $\phi = 0.1$, $Gr = 3.0$, $\epsilon = 2.5$.

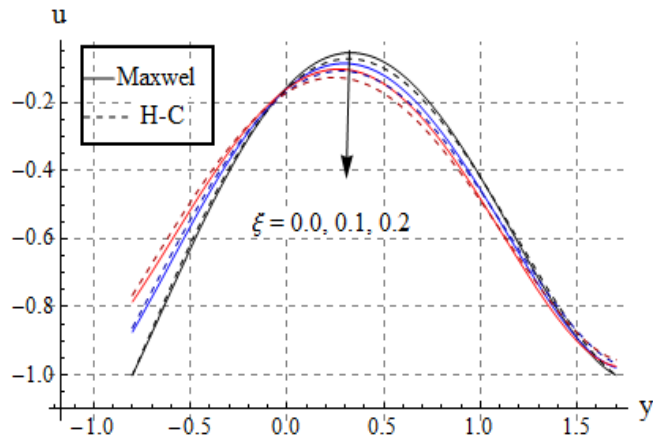


Fig. 3.12. Variation of velocity for Ag for change in velocity slip when $a = 0.7$, $b = 0.6$, $\gamma = \pi/2$, $d = 0.8$, $x = 0$, $\eta = 0.7$, $Br = 0.3$, $\zeta = 0.1$, $\phi = 0.1$, $Gr = 3.0$, $\epsilon = 2.5$.

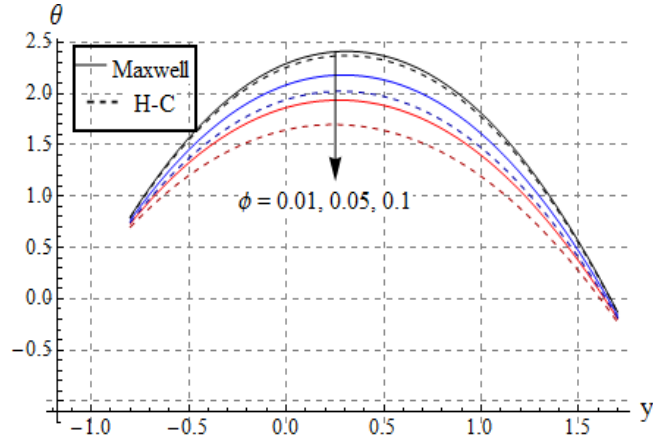


Fig. 3.13. Variation of temperature for TiO_2 for change in ϕ when $a = 0.7$, $b = 0.6$, $\gamma = \pi/2$, $d = 0.8$, $x = 0$, $\eta = 0.7$, $Br = 0.3$, $\xi = 0.1$, $\zeta = 0.1$, $Gr = 3.0$, $\epsilon = 2.5$.

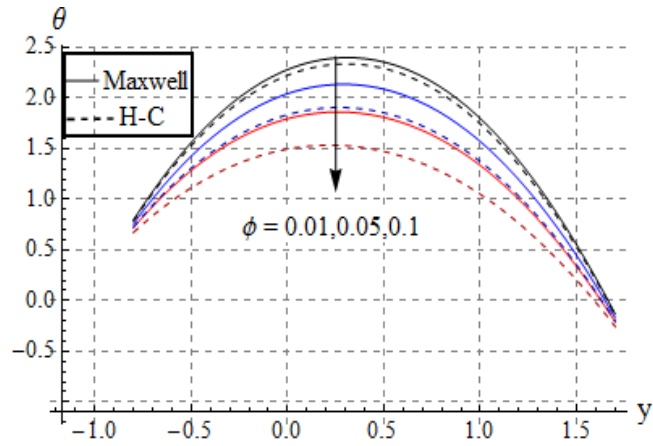


Fig. 3.14. Variation of temperature for Al_2O_3 for change in ϕ when $a = 0.7$, $b = 0.6$, $\gamma = \pi/2$, $d = 0.8$, $x = 0$, $\eta = 0.7$, $Br = 0.3$, $\xi = 0.1$, $\zeta = 0.1$, $Gr = 3.0$, $\epsilon = 2.5$.

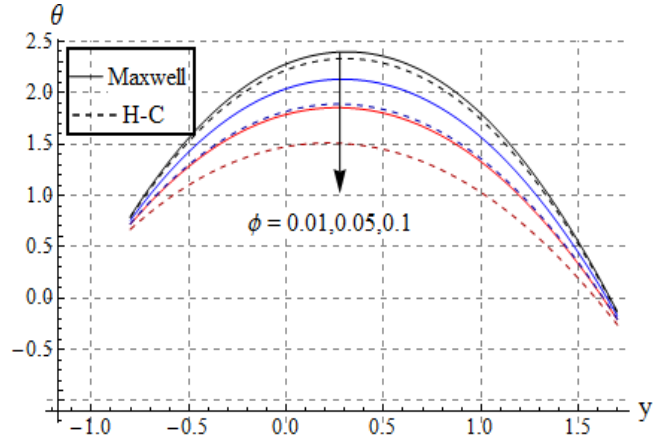


Fig. 3.15. Variation of temperature for CuO for change in ϕ when $a = 0.7$, $b = 0.6$, $\gamma = \pi/2$, $d = 0.8$, $x = 0$, $\eta = 0.7$, $Br = 0.3$, $\xi = 0.1$, $\zeta = 0.1$, $Gr = 3.0$, $\epsilon = 2.5$.

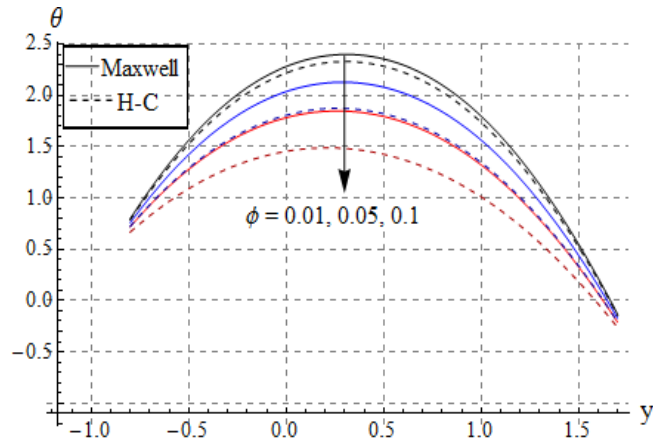


Fig. 3.16. Variation of temperature for Cu for change in ϕ when $a = 0.7$, $b = 0.6$, $\gamma = \pi/2$, $d = 0.8$, $x = 0$, $\eta = 0.7$, $Br = 0.3$, $\xi = 0.1$, $\zeta = 0.1$, $Gr = 3.0$, $\epsilon = 2.5$.

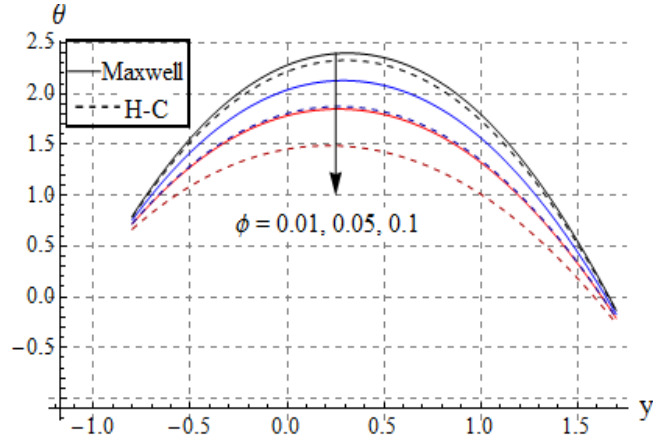


Fig. 3.17. Variation of temperature for Ag for change in ϕ when $a = 0.7$, $b = 0.6$, $\gamma = \pi/2$, $d = 0.8$, $x = 0$, $\eta = 0.7$, $Br = 0.3$, $\xi = 0.1$, $\zeta = 0.1$, $Gr = 3.0$, $\epsilon = 2.5$.

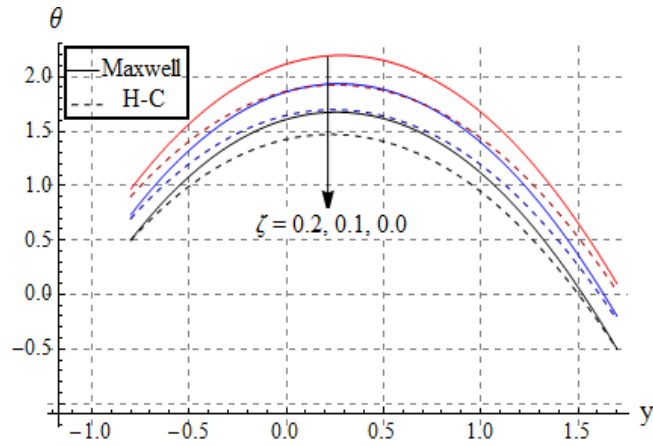


Fig. 3.18. Variation of temperature for TiO_2 for change in thermal slip when $a = 0.7$, $b = 0.6$, $\gamma = \pi/2$, $d = 0.8$, $x = 0$, $\eta = 0.7$, $Br = 0.3$, $\xi = 0.1$, $\phi = 0.1$, $Gr = 3.0$, $\epsilon = 2.5$.

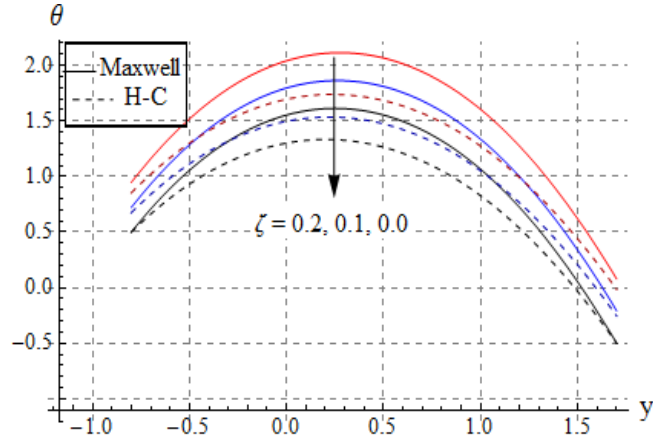


Fig. 3.19. Variation of temperature for Al_2O_3 for change in thermal slip when $a = 0.7$, $b = 0.6$, $\gamma = \pi/2$, $d = 0.8$, $x = 0$, $\eta = 0.7$, $Br = 0.3$, $\xi = 0.1$, $\phi = 0.1$, $Gr = 3.0$, $\epsilon = 2.5$.

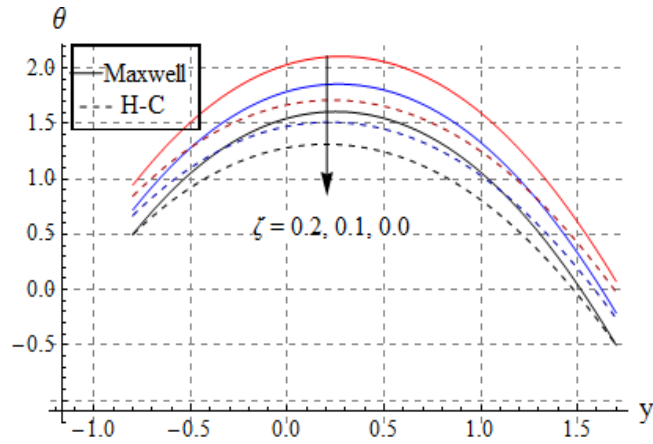


Fig. 3.20. Variation of temperature for CuO for change in thermal slip when $a = 0.7$, $b = 0.6$, $\gamma = \pi/2$, $d = 0.8$, $x = 0$, $\eta = 0.7$, $Br = 0.3$, $\xi = 0.1$, $\phi = 0.1$, $Gr = 3.0$, $\epsilon = 2.5$.

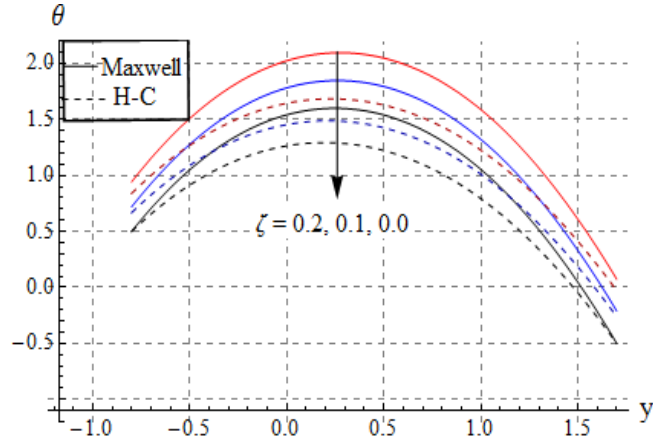


Fig. 3.21. Variation of temperature for Cu for change in thermal slip when $a = 0.7$, $b = 0.6$, $\gamma = \pi/2$, $d = 0.8$, $x = 0$, $\eta = 0.7$, $Br = 0.3$, $\xi = 0.1$, $\phi = 0.1$, $Gr = 3.0$, $\epsilon = 2.5$.

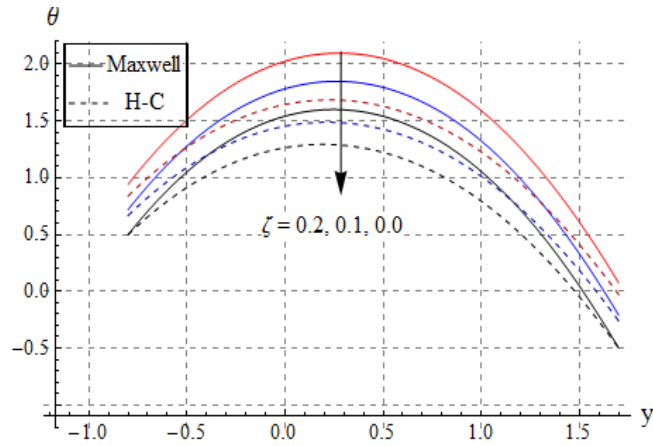


Fig. 3.22. Variation of temperature for Ag for change in thermal slip when $a = 0.7$, $b = 0.6$, $\gamma = \pi/2$, $d = 0.8$, $x = 0$, $\eta = 0.7$, $Br = 0.3$, $\xi = 0.1$, $\phi = 0.1$, $Gr = 3.0$, $\epsilon = 2.5$.

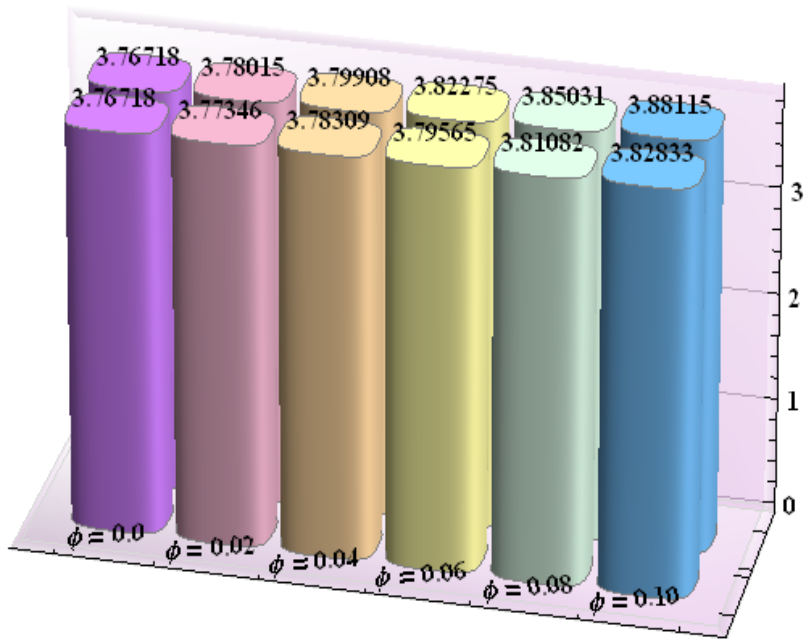


Fig. 3.23. Change via nanoparticle volume fraction in heat transfer rate at the wall $(-\frac{K_{eff}}{K_f}\theta'(h_1))$ for TiO₂ -water nanofluid when $a = 0.7$, $b = 0.6$, $\gamma = \pi/2$, $d = 0.8$, $x = 0$, $\eta = 0.7$, $Br = 0.3$, $\xi = 0.1$, $\zeta = 0.1$, $Gr = 3.0$, $\epsilon = 2.5$.

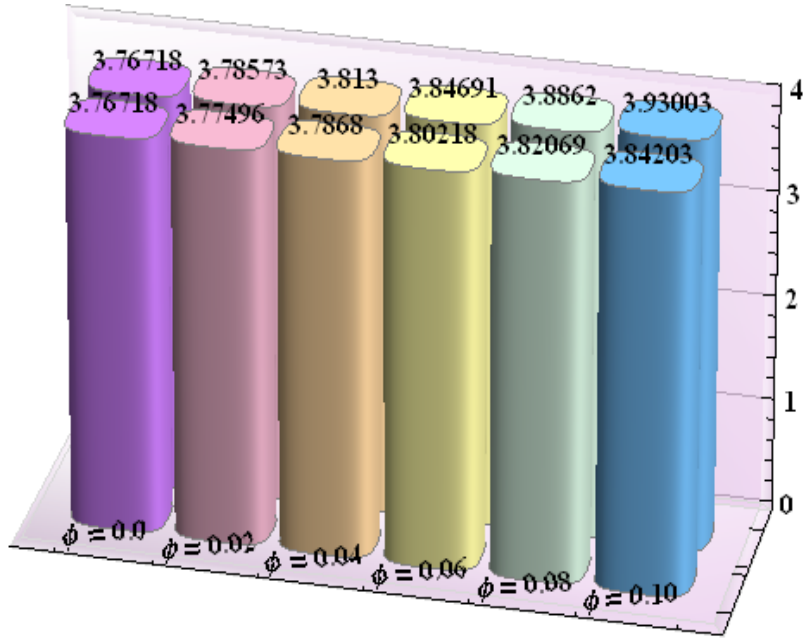


Fig. 3.24. Change via nanoparticle volume fraction in heat transfer rate at the wall $(-\frac{K_{eff}}{K_f}\theta'(h_1))$ for Al_2O_3 -water nanofluid when $a = 0.7$, $b = 0.6$, $\gamma = \pi/2$, $d = 0.8$, $x = 0$, $\eta = 0.7$, $Br = 0.3$, $\xi = 0.1$, $\zeta = 0.1$, $Gr = 3.0$, $\epsilon = 2.5$.

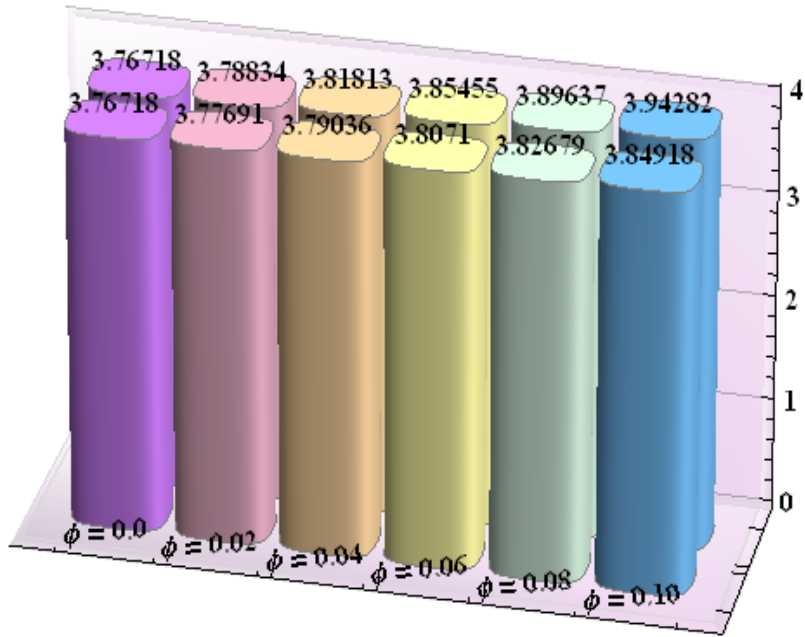


Fig. 3.25. Change via nanoparticle volume fraction in heat transfer rate at the wall $(-\frac{K_{eff}}{K_f}\theta'(h_1))$ for CuO- water nanofluid when $a = 0.7$, $b = 0.6$, $\gamma = \pi/2$, $d = 0.8$, $x = 0$, $\eta = 0.7$, $Br = 0.3$, $\xi = 0.1$, $\zeta = 0.1$, $Gr = 3.0$, $\epsilon = 2.5$.

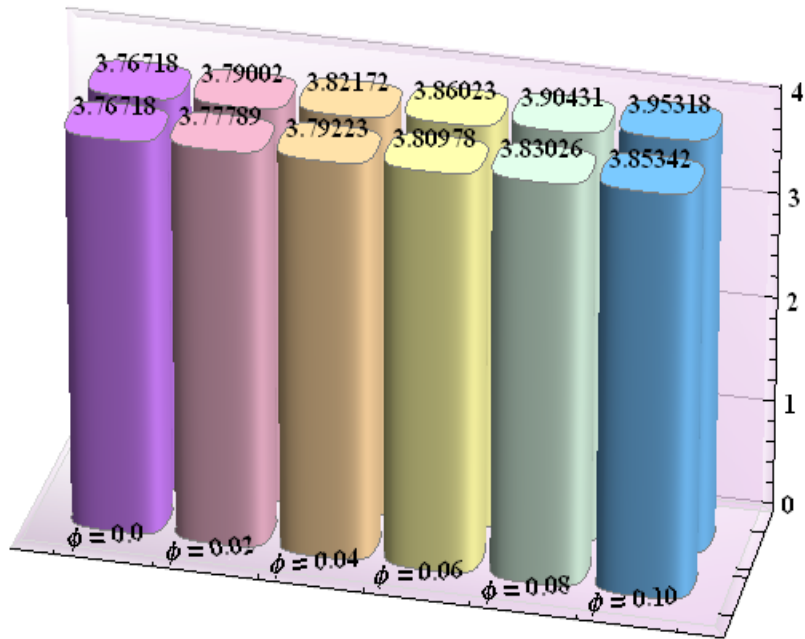


Fig. 3.26. Change via nanoparticle volume fraction in heat transfer rate at the wall $(-\frac{K_{eff}}{K_f}\theta'(h_1))$ for Cu-water nanofluid when $a = 0.7$, $b = 0.6$, $\gamma = \pi/2$, $d = 0.8$, $x = 0$, $\eta = 0.7$, $Br = 0.3$, $\xi = 0.1$, $\zeta = 0.1$, $Gr = 3.0$, $\epsilon = 2.5$.

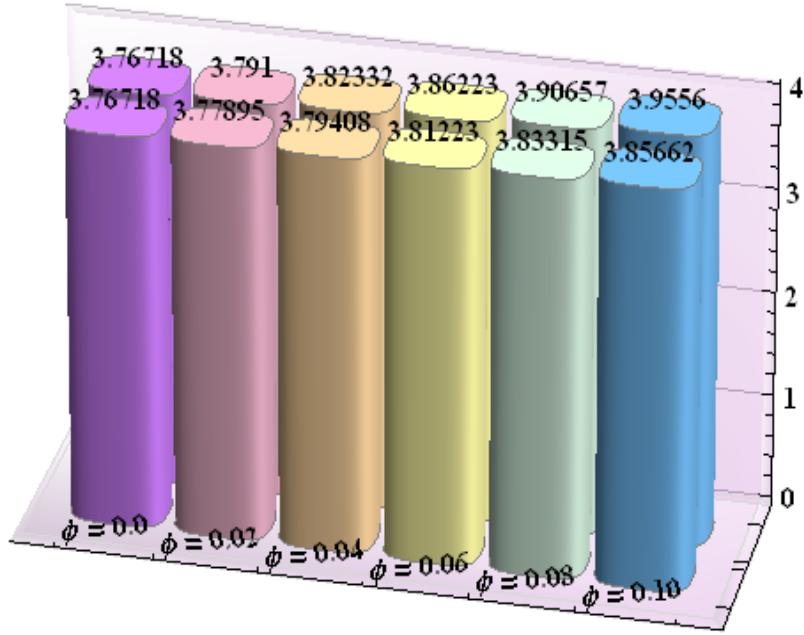


Fig. 3.27. Change via nanoparticle volume fraction in heat transfer rate at the wall $(-\frac{K_{eff}}{K_f}\theta'(h_1))$ for Ag-water nanofluid when $a = 0.7$, $b = 0.6$, $\gamma = \pi/2$, $d = 0.8$, $x = 0$, $\eta = 0.7$, $Br = 0.3$, $\xi = 0.1$, $\zeta = 0.1$, $Gr = 3.0$, $\epsilon = 2.5$.

3.4 Conclusions

Here consideration is given to the mixed convection peristaltic transport of water based nanofluids with velocity and thermal slip conditions in an asymmetric channel. The main observations of the analysis are:

- By adding the nanoparticles, fluid's maximum velocity decreases.
- Increase in velocity slip parameter decreases the velocity of the nanofluid near the center of channel.
- Thermal slip parameter and nanoparticles volume fraction ϕ show opposite behavior for temperature θ .

- The heat transfer rate at the walls is enhanced when the nanoparticles with high thermal conductivity are used.
- Greater values of heat transfer for Hamilton-Crosser's model than the Maxwell's model shows that the cylindrical shaped nanoparticles enhanced the heat transfer rate more than the spherical shaped nanoparticles.
- The difference of values of the two models widens when we increase the nanoparticles volume fraction.

Bibliography

- [1] S. U. S. Choi, Enhancing thermal conductivity of the fluids with nanoparticles, ASME Fluids Eng. Div., 231 (1995) 99-105.
- [2] K. Khanafer, K. Vafai and M. Lightstone, Buoyancy-driven heat transfer enhancement in a two dimensional enclosure utilizing nanofluids, Int J. Heat Mass Transfer, 46 (2003) 3639-3653.
- [3] J. Buongiorno, Convective transport in nanofluids, ASME J. Heat Transfer, 128 (2006) 240-250.
- [4] J. Buongiorno, D. C. Venerus and N. Prabhat et.al, A benchmark study on the thermal conductivity of nanofluids, J. Appl. Phys., 106 (2009) Articles ID 094312.
- [5] A. Ghadimi, R. Saidur and H. S. C. Metselaar, A review of nanofluids stability properties and characterization in stationary conditions, Int. J. Heat Mass Transfer, 54 (2011) 4051-4068.
- [6] I. M. Mahbubul, R. Saidur and M. A. Amalina, latest developments on the viscosity of nanofluids, Int. J. Heat Mass Transfer, 55 (2012) 874-885.
- [7] K. Khanafer and K. Vafai, A critical synthesis of thermophysical characteristics of nanofluids, Int. J. Heat Mass Transfer, 54 (2011) 4410-4428.
- [8] Z. Alloui, P. Vasseur and M. Reggio, Natural convection of nanofluids in a shallow cavity heated from below, Int. J. Therm. Sci., 50 (2011) 385-393.

- [9] M. Turkyilmazoglu, The analytical solution of mixed convection heat transfer and fluid flow of a MHD viscoelastic fluid over a permeable stretching surface, *Int. J. Mech. Sci.*, 77 (2013) 263–268.
- [10] M. Turkyilmazoglu, Nanofluid flow and heat transfer due to a rotating disk, *Comput. Fluids*, 94 (2014) 139–146.
- [11] M. Sheikholeslami, M. Gorji-Bandpy, D. D. Ganji and S. Soleimani, Heat flux boundary condition for nanofluid filled enclosure in presence of magnetic field, *J. Mol. Liq.*, 193 (2014) 174–184.
- [12] M. Sheikholeslami and D. D. Ganji, Nanofluid flow and heat transfer between parallel plates considering Brownian motion using DTM, *Comput. Methods Appl. Mech. Eng.*, 283 (2015) 651–663.
- [13] M. Sheikholeslami, D. D. Ganji, M. Y. Javed and R. Ellahi, Effect of thermal radiation on magnetohydrodynamics nanofluid flow and heat transfer by means of two phase model, *J. Magn. Magn. Mater.*, 374 (2015) 36–43.
- [14] M. Lomascolo, G. Colangelo, M. Milanese and A. Risi, Review of heat transfer in nanofluids: conductive, convective and radiative experimental results, *Renewable Sustainable Energy Rev.*, 43 (2015) 1182–1198.
- [15] A. H. Shapiro, Pumping and retrograde diffusion in peristaltic waves, In *Proc. Workshop Ureteral Reftm Children*, Nat. Acad. Sci., Washington, DC, 1 (1967) 109–126.
- [16] S. L. Weinberg, Theoretical and experimental treatment of peristaltic pumping and its relation to ureteral function, Ph.D. Thesis, MIT, Cambridge, MA, (1970).
- [17] S. Asghar, Q. Hussain, and T. Hayat, Peristaltic motion of reactive viscous fluid with temperature dependent viscosity, *Math. Comp. App.*, 18 (2013) 198–220.
- [18] Kh. S. Mekheimer, Y. A. Elmaboud and A. I. Abdellateef, Particulate suspension flow induced by sinusoidal peristaltic waves through eccentric cylinders: thread annular, *Int. J. Biomath.*, 06 (2013) 1350026.

- [19] S. Akram, S. Nadeem and M. Hanif, Numerical and analytical treatment on peristaltic flow of Williamson fluid in the occurrence of induced magnetic field, *J. Magn. Magn. Mater.*, 346 (2013) 142-151.
- [20] S. Hina, M. Mustafa, T. Hayat and F. E. Alsaadi, Peristaltic motion of third grade fluid in curved channel, *App. Math. Mech-Engl, Ed.*, 35 (2014) 73-84.
- [21] T. Hayat, F. M. Abbasi, B. Ahmad and A. Alsaedi, Peristaltic transport of Carreau–Yasuda fluid in a curved channel with slip effects, *PLoS One*, 9 (2014) e95070.
- [22] M. Mustafa, S. Hina, T. Hayat and B. Ahmad, Influence of induced magnetic field on the peristaltic flow of nanofluid, *Meccan.*, 49 (2014) 521-534.
- [23] S. Noreen and M. Qasim, Influence of Hall Current and viscous dissipation on pressure driven flow of pseudoplastic fluid with heat generation: A mathematical study *PLoS One*, 10 (2015) e0129588.
- [24] F. M. Abbasi, T. Hayat and A. Alsaedi, Numerical analysis for MHD peristaltic transport of Carreau–Yasuda fluid in a curved channel with Hall effects, *J. Magn. Magn. Mater.*, 382 (2015) 104–110.
- [25] M. Kothandapani and J. Prakash, Effect of thermal radiation parameter and magnetic field on the peristaltic flow of Williamson nanofluids in a tapered asymmetric channel, *Int. J. Heat Mass Transfer*, 51 (2015) 234-245.
- [26] T. Hayat, M. Rafiq and B. Ahmad, Combined effects of rotation and thermal radiation on peristaltic transport of Jeffrey fluid, *Int. J. Biomath.*, 8 (2015) 21.
- [27] T. Hayat, M. Rafiq and B. Ahmad, Radiative and Joule heating effects on peristaltic transport of dusty fluid in a channel with wall properties, *Eur. Phys. J. Plus*, 129 (2015) 225.
- [28] S. Noreen, T. Hayat, A. Alsaedi and M. Qasim, Mixed convection heat and mass transfer in the peristaltic flow with chemical reaction and inclined magnetic field. *Indian J. Phys.*, 87 (2013) 889–896.

- [29] O.U. Mehmood, N. Mustapha and S. Shafie, Heat transfer on peristaltic flow of fourth grade fluid in inclined asymmetric channel with partial slip. *Appl. Math. Mech. -Engl. Ed.*, 33 (2012) 1313–1328.
- [30] S. Hina, M. Mustafa, T. Hayat and N. D. Alotaibi, On the peristaltic motion of pseudo-plastic fluid in a curved channel with heat/mass transfer and wall properties, *App. Math. Comp.*, 263 (2015) 378-391.
- [31] T. Hayat, S. Noreen, M. Alhothuali, S. Asghar and A. Alhomaiddan, Peristaltic flow under the effects of an induced magnetic field and heat and mass transfer. *Int. J. Heat Mass Transfer*, 55 (2012) 443–452.
- [32] Kh. S. Mekheimer, SZA. Husseny and YA. Elmaboud, Effects of heat transfer and space porosity on peristaltic flow in a vertical asymmetric channel. *Numer. Methods Partial Diff. Eqs.*, 26 (2010) 747–770.
- [33] T. Hayat, S. Noreen and M. Qasim , Influence of heat and mass transfer on the peristaltic transport of Phan-Thien- Tanner fluid. *ZNA.*, 68a (2013) 751–758.
- [34] F. M. Abbasi, T. Hayat and B. Ahmad, Impact of magnetic field on mixed convective peristaltic flow of water based nanofluids with Joule heating, *Z. Naturforsch.*, 70 (2015) 125–132 (a).
- [35] F. M. Abbasi, T. Hayat and B. Ahmad, Peristaltic transport of copper-water nanofluid saturating porous medium, *Physica E*, 67 (2015) 47–53.
- [36] F. M. Abbasi, T. Hayat and A. Alsaedi, Peristaltic transport of magneto-nanoparticles submerged in water: model for drug delivery system, *Physica E*, 68 (2015) 123–132.
- [37] F. M. Abbasi, T. Hayat and B. Ahmad, Peristaltic flow in an asymmetric channel with convective boundary conditions and Joule heating, *J. Cent. South Univ.*, 21 (2014) 1411–1416.
- [38] S. A. Shehzad, F. M. Abbasi, T. Hayat and F. Alsaadi, Model and comparative study for the peristaltic transport of water based nanofluids, *J. Mol. Liq.*, 209 (2015) 723–728.

- [39] F. M. Abbasi, T. Hayat, B. Ahmad and G. Q. Chen, Peristaltic motion of non-Newtonian nanofluid in an asymmetric channel, *Z. Naturforsch.*, 69a (2014) 451–461.
- [40] S. A. Shehzad, F. M. Abbasi, T. Hayat and F. Alsaadi, MHD mixed convective peristaltic motion of nanofluid with Joule heating and thermophoresis effects, *PLoS One*, 9 (2014) e111417.
- [41] T. Hayat, F. M. Abbasi, M. Al-Yami and S. Monaquel, Slip and Joule heating effects in mixed convection peristaltic transport of nanofluid with Soret and Dufour effects, *J. Mol. Liq.*, 194 (2014) 93–99.
- [42] F. M. Abbasi, T. Hayat, B. Ahmad and G. Q. Chen, Slip effects on mixed convective peristaltic transport of copper-water nanofluid in an inclined channel, *PLoS One*, 9 (2014) e105440.
- [43] F. M. Abbasi, T. Hayat and B. Ahmad, Peristalsis of silver-water nanofluid in the presence of Hall and Ohmic heating effects: applications in drug delivery, *J. Mol. Liq.*, 207 (2015) 248–255.
- [44] J. C. Maxwell, *A Treatise on Electricity and Magnetism*, 2nd Edition Oxford University Press, Cambridge, (1904) 435–441.
- [45] R. L. Hamilton and O. K. Crosser, Thermal conductivity of heterogeneous two component systems, *EC Fundam.*, 1 (1962) 187–191.